Masters Theses   Graduate School

8-2020

Extracellular Enzymes in Aquatic Environments: Possible Role of Non-Specific Peptidases in Microcystin Degradation and Effects of Assay Protocol on Calculated Activities

Christopher Cook
University of Tennessee

Follow this and additional works at: https://trace.tennessee.edu/utk_gradthes

To the Graduate Council:

I am submitting herewith a thesis written by Christopher Cook entitled "Extracellular Enzymes in Aquatic Environments: Possible Role of Non-Specific Peptidases in Microcystin Degradation and Effects of Assay Protocol on Calculated Activities." I have examined the final electronic copy of this thesis for form and content and recommend that it be accepted in partial fulfillment of the requirements for the degree of Master of Science, with a major in Geology.

<div align="right">Andrew Steen, Major Professor</div>

We have read this thesis and recommend its acceptance:

Annette Engel, Steven Wilhelm

<div align="right">Accepted for the Council:
Dixie L. Thompson</div>

<div align="right">Vice Provost and Dean of the Graduate School</div>

(Original signatures are on file with official student records.)

**EXTRACELLULAR ENZYMES IN AQUATIC ENVIRONMENTS:
POSSIBLE ROLE OF NON-SPECIFIC PEPTIDASES IN
MICROCYSTIN DEGRADATION AND EFFECTS OF ASSAY
PROTOCOL ON CALCULATED ACTIVITIES**

**A Thesis Presented for the
Master of Science
Degree
The University of Tennessee, Knoxville**

**Christopher Lee Cook
August 2020**

DEDICATION

I dedicate this work to my dog and friend of sixteen years.
Farewell, Godzilla.

ACKNOWLEDGEMENTS

ABSTRACT

Extracellular enzyme assays are widely used methods to probe the interactions between microbes and complex organic matter. Microbes produce extracellular enzymes to degrade macromolecules into smaller molecules that can be transported across cell membranes. Enzyme assays provide a quantitative understanding of the rates and specificities of extracellular enzymes toward these macromolecules. This study explored 1) the biodegradation pathways of microcystin-LR (MC-LR), a cyanobacterial peptide toxin, by measuring the activities of extracellular peptidases produced by putative MC-LR degraders and 2) the effects of enzyme assay protocol on activity measurements, which involved the creation of *ezmmek*, an R package designed to analyze enzyme assay data reproducibly under different protocols. *Lactobacillus rhamnosus* GG, an MC-LR degrader that employs an unknown pathway, produces L-Leucine aminopeptidases. Future work can test whether these same peptidases are capable of degrading MC-LR. Two enzyme assay protocols were applied to the same freshwater sample, but resulted in significantly different activity measurements when analyzed with *ezmmek*. Widespread adoption of *ezmmek* could standardize enzyme analytical pathways performed by other researchers, and will make results more comparable among MC-LR and other organic matter degradation studies.

TABLE OF CONTENTS

LIST OF FIGURES

LIST OF *ezmmek* FUNCTIONS

CHAPTER I
INTRODUCTION

Microcystin-LR

Impacts on Human and Ecosystem Health

Microcystin (MC), an intracellular hepatotoxin produced as a secondary metabolite by several genera of cyanobacteria in freshwater and marine environments, can poison drinking water and damage ecosystems. Dangerous concentrations of MC typically accompany certain species of cyanobacterial cells present in high abundances, i.e. harmful cyanobacterial blooms (Huisman et al., 2018). Such events force the shutdown of drinking water sources for days at a time, and leave thousands of people without access to tap water (Qin et al., 2009). MC also impairs ecosystems by affecting bacteria, plants, and invertebrates (Zanchett & Oliveira-Filho, 2013). Acute exposure to MC can be lethal to a variety of fish species (Rohrlack et al., 2005). Chronic exposure has been linked to a reduction in fertility and growth rates in aquatic life (Zanchett & Oliveira-Filho, 2013). Cyanobacterial bloom formation, and subsequently MC production, are likely to increase in the future due to higher levels of eutrophication and warmer temperatures associated with climate change (Paerl et al., 2016). MC poses significant threats to both human and ecosystem health, which makes its degradation mechanisms important to the scientific community.

Production and Degradation Mechanisms

The biological functions of MC are a mystery, although some researchers hypothesize it may have once served as an anti-grazing mechanism (Codd, 1995). Although MC has over 250 structural variants (Bouaïcha et al., 2019), all of them take the form of a cyclic heptapeptide. Two of the amino acids, located at positions 2 and 4 in the ring, dictate most of the structural variability between types of MC. MC-LR ($C_{49}H_{74}N_{10}O_{12}$) is the most common variant (Merwe, 2015) and contains L-Leucine and L-Arginine in these positions (Figure I-1). The stable ring structure renders MC-LR resistant to the common physical degradation mechanisms of high temperature, extreme pH, and sunlight (Tsuji et al., 1994; Gagala & Mankiewicz-Boczek, 2012; Rastogi et al., 2014). The presence of several uncommon amino acids, such as those with the D-isomeric form, also render MC-LR resistant to many biodegradation mechanisms. Break-down by microcystinase, a group of extracellular enzymes that first cleave the ring structure at the 3-amino-9-methyoxy-2,6,8-trimethyl-10-phenyl-4,6-decadienoic acid (ADDA)-arginine bond, is the only proven pathway for the biodegradation of MC-LR and some other structural variants of MC (Figure I-2; Schmidt et al., 2014)

Biodegradation by Non-Specific Pathways

Although break-down by microcystinase is the only proven pathway, several phylogenetically diverse microbes have been discovered that can degrade MC-LR, despite lacking the genes necessary to express microcystinase (Li et al., 2017). However, the pathways performed by these microbes are unknown (Li et al., 2017). We propose that MC-LR can be biodegraded through a variety of non-specific pathways induced by

2

extracellular enzymes. Here, a non-specific pathway is defined as one that may possess some ability to degrade MC-LR, but only as a secondary function. Microbes across the phylogenetic tree produce extracellular peptidases, and some peptidases express broad substrate specificity in aquatic environments (Steen et al., 2015). Evidence for non-specific degradation may further our knowledge of MC-LR degradation in the environment as well as assist in the development of novel bioremediation practices.

Extracellular Enzyme Assays

Michaelis-Menten Kinetics

Heterotrophic bacteria produce extracellular enzymes to degrade peptides that allows them to assimilate nutrients. Most environmental enzymes, including aminopeptidases, exhibit Michaelis-Menten kinetics (Gonzales & Robert-Baudouy, 1996). Michaelis-Menten kinetics is a model used to predict changes in enzymatic activity as a function of substrate concentration, and can be described mathematically as:

$$(\text{I-1}) \quad V_0 = \frac{V_{max} * [\text{S}]}{[\text{S}] + K_M}$$

where V_0 is the rate of reaction or activity, V_{max} is the maximum rate of reaction, [S] is the concentration of substrate, and K_M is the concentration of substrate at which $V_0 = \frac{1}{2} V_{max}$ (Figure I-3). The K_M value describes the affinity of enzymes toward a particular substrate and behaves independently of cell count or sample volume. Furthermore, K_M values provide a quantitative means to compare enzyme affinities of several samples toward a variety of substrates.

Application to Ecosystem Studies

Extracellular enzyme assays are widely used tools to describe the Michaelis-Menten kinetics of extracellular enzymes present in environmental samples. Fluorometric assays, a common and straightforward technique, involve the exposure of the sample to a fluorogenic substrate proxy. A fluorogenic substrate proxy consists of a substrate bonded to a fluorophore that only fluoresces once that bond is cleaved (Figure I-4). Fluorescence increases as enzymes cleave and release more of the fluorophore over time. The bond that is cleaved is assumed to be analogous to the bond of a natural substrate that those enzymes might cleave. A standard curve consisting of free fluorophore can be used to convert fluorescence to concentration of fluorophore. Activity can be described as the concentration of fluorophore released over time per unit of volume or mass. In this study, fluorometric enzyme assays were applied to substrate proxies thought to represent similar peptide bonds present in MC-LR, with the goal of identifying unknown biodegradation pathways.

At present, a singular fluorometric enzyme assay protocol is not applied universally among studies. Studies differ in how they correct for fluorometric quenching, which in turn affects how enzymatic activities are calculated. To stimulate discussion about how to best optimize fluorometric enzyme assays, we developed *ezmmek* (Easy Michaelis-Menten Enzyme Kinetics), an R package designed to analyze fluorometric enzyme assay data according to different protocols. *ezmmek* was used to compare enzymatic activity measurements of the same freshwater sample using two protocols found in the literature. A standardized and universal approach to fluorometric enzyme assays may benefit those researching MC-LR or other organic matter degradation by

making data comparable across several studies and experiments. At the very least, the

practitioners of these studies may benefit from explicitly stating how their enzyme assays

were performed.

References

Berg J.M., Tymoczko J.L., & Stryer, L. (2002). *Biochemistry*. 5th edition. New York: W.H. Freeman. Section 8.4, The Michaelis-Menten Model Accounts for the Kinetic Properties of Many Enzymes. Available from: https://www.ncbi.nlm.nih.gov/books/NBK22430/

Bouaïcha, N., Miles, C.O., Beach. D.G. Labidi, Z., Djabri, A., Benayache, N.Y, & Nguyen-Quang, T. (2019). Structural diversity, characterization, and toxicology of microcystins. *Toxins 11*, 714.

Codd, G.A. (1995). Cyanobacterial toxins: Occurrence, properties, and biological significance. *Water Science and Technology, 32*(4), 149-156

Gagala, I. & Mankiewicz-Boczek, J. (2012). The natural degradation of microcystins (cyanobacteria hepatotoxins) in fresh water – the future of modern treatment systems and water quality improvement. *Polish Journal of Environmental Studies, 21*(5), 1125-1139.

Gonzales, T. & Robert-Baudouy, J. (1996). Bacterial aminopeptidases: Properties and functions. *FEMS Microbiology Reviews, 18*(4), 319-344.

Huisman, J., Paerl, H.W., Codd, G.A., & Visser, P.M. (2018). Cyanobacterial blooms. *Nature Reviews in Microbiology 16*(8), 471-483.

Li, J., Li, R., & Li, J. (2017). Current research scenario for microcystins biodegradation – A review on fundamental knowledge, application prospects and challenges. *Science of the Total Environment, 595,* 615-632.

Merwe, D. (2015). Cyanobacterial (Blue-Green Algae) Toxins. In: R.C. Gupta, *Handbook of Toxicology of Chemical Warfare Agents*.

Paerl, H.W., Scott, J.T., McCarthy, M.J., Newell, S.E., Gardner, W.S., Havens, K.E.,

    Hoffman, D.K., Wilhelm, S.W., & Wurtsbaugh, W.A. (2016). Mitigating

    cyanobacterial harmful algal blooms in aquatic ecosystems impacted by climate

    change and anthropogenic nutrients. *Harmful Algae, 54*, 213-222.

Qin, B., Zhu, G., Gao, G., Zhang, Y., Li, W., Paerl, H.W., & Carmichael, W.W. (2009).

    A drinking water crisis in Lake Taihu, China: linkage to climatic variability and

    lake management. *Environmental Management, 45*(1), 105-112.

Rastogi, R.P., Sinha, R.P., & Incharoensakdi, A. (2014). The cyanotoxin-microcystins:

    current overview. *Environmental Science and Biotechnology, 13*, 215-249.

Rohrlack, T., Christoffersen, K., Dittmann, E., Nogueira, I., Vasconcelos, V., & Börner,

    T. (2005). Ingestion of microcystins by *Daphnia*: Intestinal uptake and toxic effects.

    Limnology and Oceanography, 50(2), 440-448.

Schmidt, J.R., Wilhelm, S.W., & Boyer, G.L. (2014). The fate of microcystins in the

    environment and challenges for monitoring. *Toxins, 6,* 3354-3387.

Steen, A.D., Vazin, J.P., Hagen, S.M., Mulligan, K.H., & Wilhelm, S.W. (2015).

    Substrate specificity of aquatic extracellular peptidases assessed by competitive

    inhibition assays using synthetic substrates. *Aquatic Microbial Ecology, 75*(3), 271–

    281.

Tsuji, K., Naito, S., Kondo, F., Ishikawa, N., Watanabe, M.F., Suzuki, M., & Harada, K.

    (1994). Stability of microcystins from cyanobacteria: Effect of light on

    decomposition and isomerization. *Environmental Science and Technology, 28*, 173-

    177.

Zanchett, G. & Oliveira-Filho, E.C. (2013). Cyanobacteria and cyanotoxins: From

impacts on aquatic ecosystems and human health to anticarcinogenic effects. *Toxins*

(Basel), *5*(10), 1896-1917.

Appendix
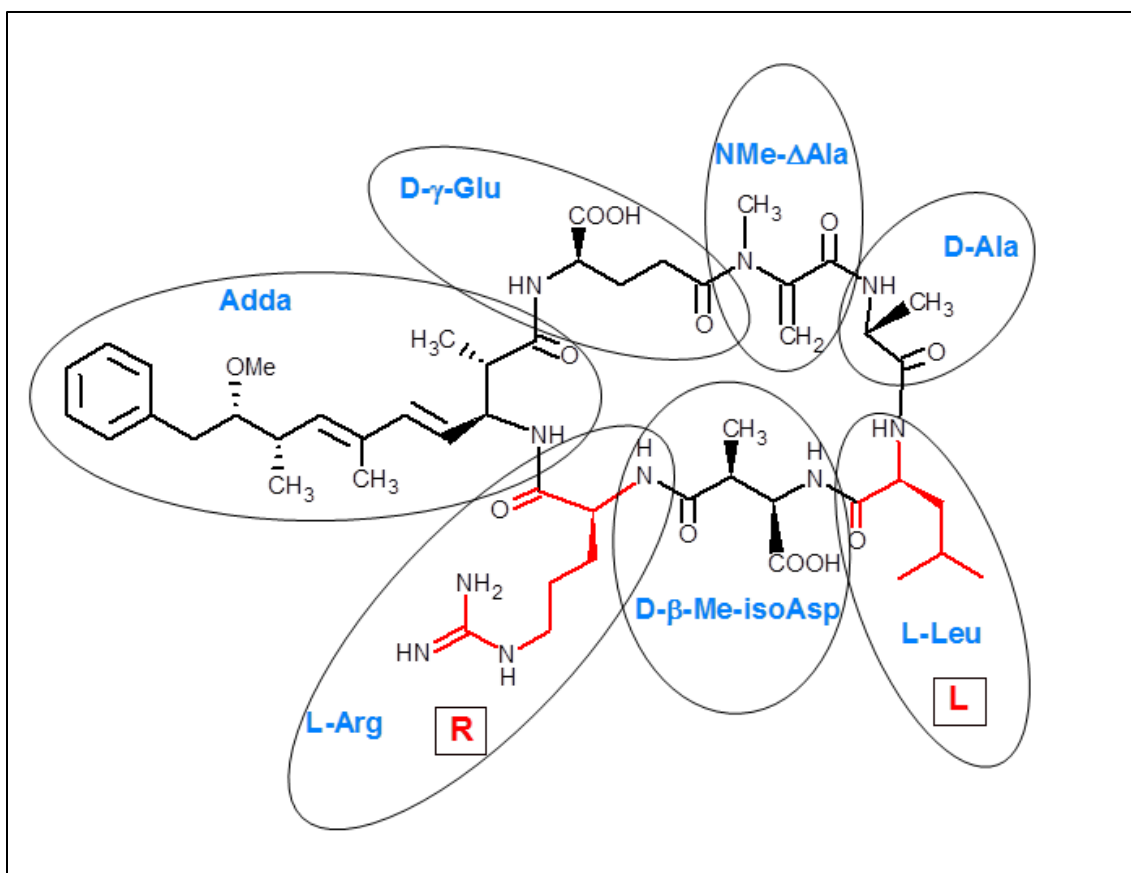
Figure I-1: Structure of Microcystin-LR.

Positions 2 and 4 (red) dictate the structural variability of MC.
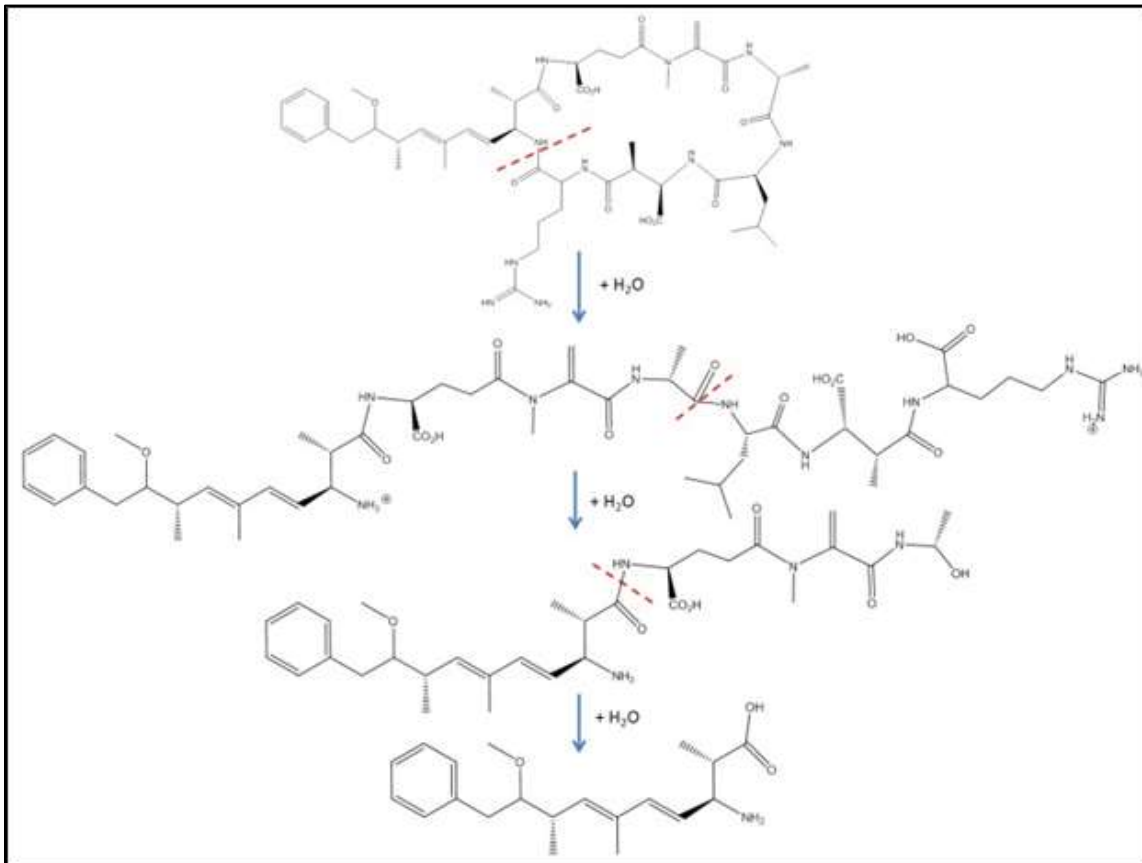
Figure I-2: Microcystinase pathway for MC-LR degradation.

The ring is cleaved via hydrolysis at the ADDA-arginine bond before being linearized

and broken down through additional hydrolysis reactions. From Schmidt et al. (2014).
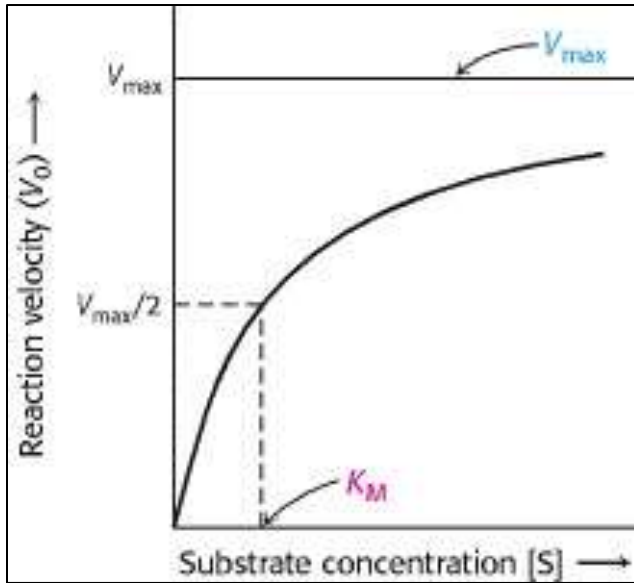
Figure I-3: Plot depiction of Michaelis-Menten Kinetics.

V_{max} is indicative of saturating conditions, and is the maximum velocity an enzymatic

reaction can achieve. From Berg et al. (2002).
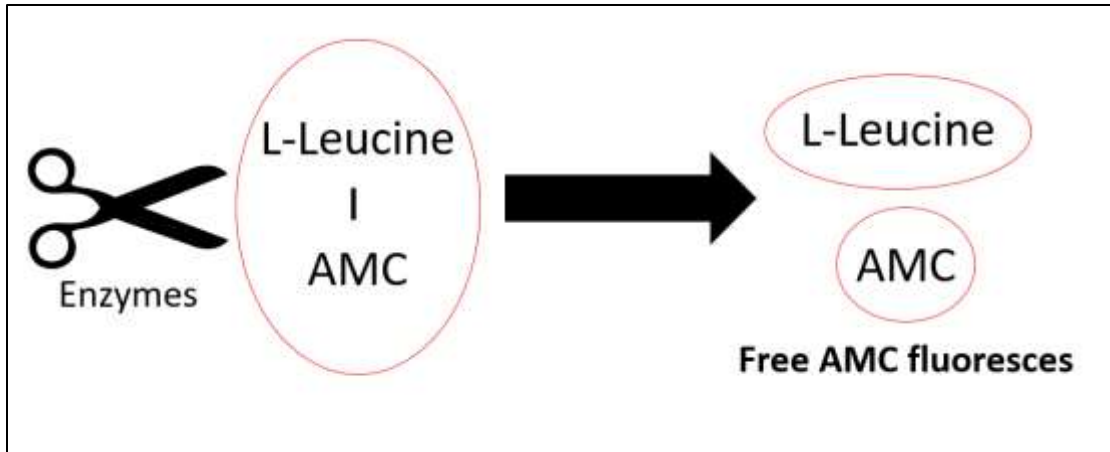
Figure I-4: Fluorometric enzyme assay schematic.

L-Leucine-7-amido-4methylcoumarin (L-Leucine-AMC) is a substrate proxy for peptide bonds attached to L-Leucine. AMC is a fluorophore that only fluoresces once cleaved from the L-Leucine. Fluorescence increases over time, as more bonds are broken through enzymatic hyrdolysis.

CHAPTER II
PEPTIDASES PRODUCED BY PUTATIVE MICROCYSTIN-LR DEGRADERS

Abstract

Microcystin (MC), a cyanotoxin produced by several genera of cyanobacteria, can poison drinking water sources and damage ecosystems. MC is a cyclic heptapeptide, whose stable ring structure is resistant to common physical degradation mechanisms. Break-down by microcystinase is the only proven pathway for the biodegradation of MC-LR, the most common structural variant of MC. However, diverse microbes that apparently lack the microcystinase enzyme can also degrade MC-LR, including *Lactobacillus rhamnosus* GG, but the pathways are unknown. We propose that MC-LR can be degraded through non-specific pathways involving extracellular enzymes. We test this nonspecific pathway hypothesis through a series of incubation experiments designed to identify the pathway by which *L. rhamnosus* GG breaks down MC-LR. *L. rhamnosus* GG, among some other bacterial strains used as controls, were exposed to a fluorogenic substrate whose bond was assumed analogous for peptide bonds present in MC-LR. We concluded that *L. rhamnosus* GG produces L-Leucine aminopeptidases. Future work will test whether these same peptidases possess the ability to degrade MC-LR.

Introduction

Extracellular Peptidases in Freshwater Systems

Heterotrophic bacteria can rapidly transform organic compounds synthesized by primary producers in aquatic systems (Bai et al., 2017). These organic compounds, which can take the form of macromolecular detritus, are too large for bacteria to assimilate directly. Heterotrophic bacteria produce extracellular enzymes to break-down

16

macromolecular detritus into assimilable nutrients (Arnosti et al., 2014). MC-LR, a structurally recalcitrant cyanobacterial peptide toxin (Bourne et al., 1996), is one such macromolecule that must be broken down before its constituents can be metabolized. Some heterotrophic bacteria produce extracellular peptidases that are specifically geared toward the degradation of MC-LR (Li et al., 2017).

Evidence for Non-Specific Degradation

The current literature identifies one pathway for the biodegradation of MC-LR. This pathway involves microcystinase, a peptidase that selectively degrades MC-LR by first cleaving the ring at the 3-amino-9-methyoxy-2,6,8-trimethyl-10-phenyl-4,6-decadienoic acid (ADDA)-arginine bond (Figure I-1; Schmidt et al., 2014). Yet, Krausfeldt et al. (2019) found that microcystinase gene transcripts were absent in harmful cyanobacterial bloom samples from Lake Erie, United States/ Canada and Lake Tai, China, two bodies of water known for producing high MC-LR concentrations. Furthermore, several phylogenetically diverse microbes that lack the ability to produce microcystinase, including *L. rhamnosus* GG, have been found to degrade MC-LR. The pathways used by these microbes are unknown. *L. rhamnosus* GG is hypothesized to degrade MC-LR via cell wall associated endopeptidases (Nybom et al., 2007; Nybom et al., 2008; Nybom et al., 2012), but the exact positions at which the ring is hydrolyzed remains unknown. We hypothesize that *L. rhamnosus* GG, along with the other microbes that employ unknown pathways, degrade MC-LR using a variety of non-specific pathways. Here, a non-specific pathway is defined as one that may possess some ability to degrade MC-LR, but only as a secondary function. Microbes across the phylogenetic

tree produce extracellular peptidases, and some peptidases exhibit broad substrate specificity in aquatic environments (Steen et al., 2015). Extracellular peptidases may be able to break down MC-LR in addition to performing their primary functions. Conclusive evidence for non-specific degradation may further knowledge of the environmental fate of MC-LR as well as assist in the development of novel bioremediation techniques.

Testing for Non-specific Degradation

To test the hypothesis that *L.* rhamnosus GG degrades MC-LR via nonspecific pathways, cultures were first assayed for the production of aminopeptidases that may degrade corresponding amino acids present in MC-LR. Here, cultures were assayed for L-Leucine aminopeptidases. L-Leucine aminopeptidases cleave peptide bonds shared by L-Leucine, one of the amino acids present in MC-LR. The assay was also performed using *Sphingomonas* ACM-3962, a positive control for the microcystinase pathway (Bourne et al., 1996), and *Escherichia coli* K12, a negative control that does not produce the extracellular peptidases required to degrade macromolecular peptides like MC-LR (Chalova et al., 2009).

Methods

Incubation Parameters

Three strains of bacteria were cultured to test the production of L-Leucine aminopeptidases. *S.* ACM-3962 was grown in 30 mL of nutrient broth for 48 hours at 30 °C [degrees Celsius] and 180 revolutions per minute (rpm). *L. rhamnosus* GG was grown in 30 mL of De Man, Rogosa, and Sharpe (MRS) broth for 48 hours at 37 °C and 180 rpm. *E. coli* K12 was grown in 30 mL of Luria-Bertani (LB) broth for 24 hours at 37 °C

and 180 rpm. Each culture was then centrifuged and washed twice in 30 mL of PBS broth

with a pH ~7.5 in ambient conditions. Enzyme assays were performed immediately after

final resuspensions of cultures in PBS.

Enzyme Assays

Each culture was exposed to L-Leucine-7-amido-4-methylcoumarin

hydrochloride (L-Leucine-AMC), a fluorogenic substrate whose bond was deemed

analogous to the peptide bonds shared by L-Leucine in MC-LR. Assays were performed

according to Steen and Arnosti (2011). Standard curves were measured in the presence of

the cultures suspended in PBS. The standard curve aliquots were made in 1.5 mL plastic

cuvettes and measured using a Promega^{TM} GloMax$^®$ fluorometer. Each aliquot consisted

of 960 µL culture suspended in PBS and 40 µL of a varying ratio of dimethyl sulfoxide

(DMSO) to 7-amino-4-methylcoumarin (AMC) dissolved in DMSO, with the ratio

dependent on the desired concentration of AMC in the final solution. Final concentrations

of AMC in the standard curve aliquots were 0.0 to 4.0 µ[micro]M (micromolar), in 0.5

µM increments.

Raw fluorescence data were collected at time intervals of 0, 10, 20, 30, and 40

minutes. These aliquots were made similarly to the standard curve aliquots, but with

intact L-Leucine-AMC dissolved in DMSO instead of pure AMC dissolved in DMSO.

Final concentrations of L-Leucine-AMC in the assay aliquots were 0, 50, 100, 200, 300,

and 400 µM. Aliquots were made in triplicate. Measurements were taken using the same

fluorometer. Raw fluorescence data were calibrated to activity using the standard curves.

Results and Discussion

Enzyme Assay Data Analysis

The saturation curves and raw fluorescence data for each microbe can be found in this chapter's appendix. As expected, *E. coli* K12, the negative control, did not exhibit Michaelis-Menten kinetics on the L-Leucine AMC (Figure II-3). Although a saturation curve was fitted to the *E. coli* K12 activities, these data exhibited a linear trend, with saturating conditions predicted well-beyond the maximum substrate concentration of 400 µM. L-Leucine-AMC degraded despite that *E. coli* K12 is not known to produce extracellular peptidases, which may be due to abiotic degradation or the release of intracellular peptidases upon cell lysis. *S.* ACM-3962 and *L. rhamnosus* GG both exhibited Michaelis-Menten kinetics, with K_M values of 225.69 and 97.27 µM of L-Leucine-AMC, respectively (Figures II-1 and II-2). *L. rhamnosus* GG had a higher affinity toward L-Leucine-AMC than *S.* ACM-3962. Although K_M behaves independently of cell count, the activities themselves did not. Therefore, the activities and V_{Max} values between *L. rhamnosus* GG and *S.* ACM-3962 were not comparable from these data. Based on these data, *L. rhamnosus* GG and *S.* AMC-3962 produce L-Leucine aminopeptidases.

Combining Enzyme Assays with MC-LR Degradation Experiments

Preliminary results suggested that *L. rhamnosus* GG produced L-Leucine aminopeptidases. Further work may determine whether these peptidases are capable of degrading MC-LR. We propose a series of incubation experiments that simultaneously

measures MC-LR degradation, fluorogenic substrate degradation, and cell growth (Figure II-7). These experiments would entail exposing *L. rhamnosus* GG (as suspended in PBS) to MC-LR and taking several timepoints over a 48-hour period. At each timepoint, subsamples would be collected to measure MC-LR concentration by high performance liquid chromatography (Nybom et al., 2007), substrate degradation by fluorometry (i.e., a subsample would be exposed to L-Leucine-AMC for up to an hour at each timepoint collected), and cell growth by spectrophotometry. In these experiments, MC-LR acts as a major carbon source (priming with other carbon sources, such as glucose, may be beneficial), which allows for assumption that the majority of cell growth can be attributed to MC-LR degradation. Quantitative relationships between these three measurements may suggest that L-Leucine aminopeptidases (or any other enzymes tested) produced by *L. rhamnosus* GG are capable of degrading MC-LR. If so, then they would likely use a pathway that first cleaves the bonds between L-Leucine and the adjacent amino acids in MC-LR, which are Alanine and Aspartic Acid. Enzyme assays involving the use of substrates analogous to other amino acids present in MC-LR should be performed to further identify possible pathways performed by *L. rhamnosus* GG. Many of the amino acids in MC-LR are atypical, and analogous substrates may need to be specially synthesized to perform additional experiments.

Conclusions

L. rhamnosus GG produces L-Leucine aminopeptidases. Additional assays are necessary to identify other aminopeptidases produced by each bacterium. After which,

more robust incubation experiments involving several enzyme substrates and novel

biodegraders can further test the hypothesis of non-specific biodegradation pathways.

References

Arnosti, C., Bell, C., Moorhead, D.L., Sinsabaugh, R.L., Steen A.D., Stomberger, M.,
Wallenstein, M., Weintraub, M.N. (2014). Extracellular enzymes in terrestrial,
freshwater, and marine environments: Perspectives on system variability and
common research needs. *Biogeochemistry*, *117*(1), 5-21.

Bai, L., Cao, C., Wang, C., Xu, H., Zhang, H., Slaveykova, V.I., & Jiang, H. (2017).
Toward quantitative understanding of the bioavailability of dissolved organic matter
in freshwater lake during cyanobacteria blooming. *Environmental Science and
Technology*, *51*(11), 6018-6026.

Bourne, D.G., Jones, G. J., Blakeley, R. L., Jones, A., Negri, A. P., & Riddles, P. (1996).
Enzymatic pathway for the bacterial degradation of the cyanobacterial cyclic
peptide toxin microcystin LR. *Applied and environmental microbiology*, *62*(11),
4086-4094.

Chalova, V. I., Sirsat, S. A., O'Bryan, C. A., Crandall, P. G., & Ricke, S. C. (2009).
Escherichia coli, an intestinal microorganism, as a biosensor for quantification of
amino acid bioavailability. *Sensors (Basel, Switzerland)*, *9*(9), 7038-7057.

Li, J., Li, R., and Li, J. (2017). Current research scenario for microcystins biodegradation
– A review on fundamental knowledge, application prospects and challenges.
Science of the Total Environment, 595, 615-632.

Nybom, M.K.S., Salminen, S.J., & Meriluoto, J.A.O. (2007). Removal of microcystin-LR
by strains of metabolically active probiotic bacteria. *Federation of European
Microbiological Societies Microbiology Letters*, *270*(1), 27-33.

Nybom, M.K.S., Salminen, S.J., & Meriluoto, J.A.O. (2008). Specific strains of probiotic

    bacteria are efficient in removal of several different cyanobacterial toxins from

    solution. *Toxicon*, *52*(2), 214-220.

Nybom, M.K.S., Dziga, D., Heikkilä, J.E., Krull, T.P.J., Salminen, S.J., & Meriluoto,

    J.A.O. (2012). Characterization of microcystin-LR removal process in the presence

    of probiotic bacteria. *Toxicon, 59*(1), 171-181.

Schmidt, J.R., Wilhelm, S.W., & Boyer, G.L. (2014). The fate of microcystins in the

    environment and challenges for monitoring. *Toxins, 6*(12), 3354-3387.

Steen, A.D. &Arnosti, C. (2011). Long lifetimes of β-glucosidase, leucine

    aminopeptidase, and phosphatase in Arctic seawater. *Marine Chemistry*, *123*(1-4),

    1019-1021.

Steen, A.D., Vazin, J.P., Hagen, S.M., Mulligan, K.H., & Wilhelm, S.W. (2015).

    Substrate specificity of aquatic extracellular peptidases assessed by competitive

    inhibition assays using synthetic substrates. *Aquatic Microbial Ecology, 75*(3), 271-

    281.

Appendix
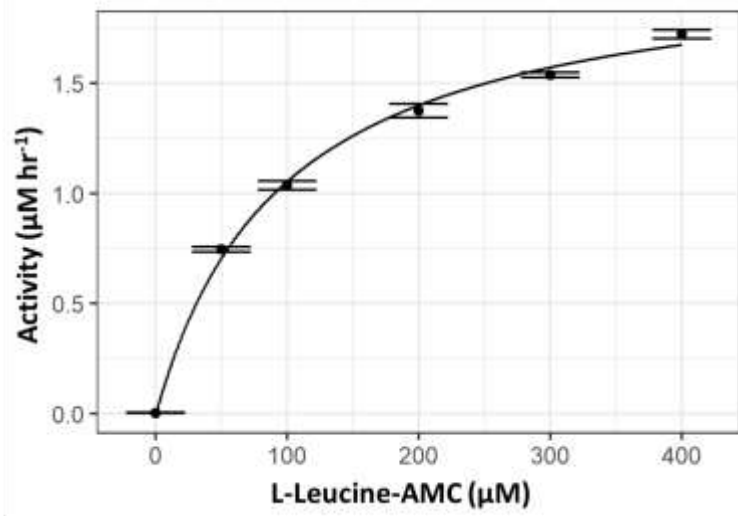
Figure II-1: Saturation curve of *L. rhamnosus* GG acting on L-Leucine-AMC.

Presented are the average activities (points) and standard deviations (error bars) of three

replicates at each substrate concentration.
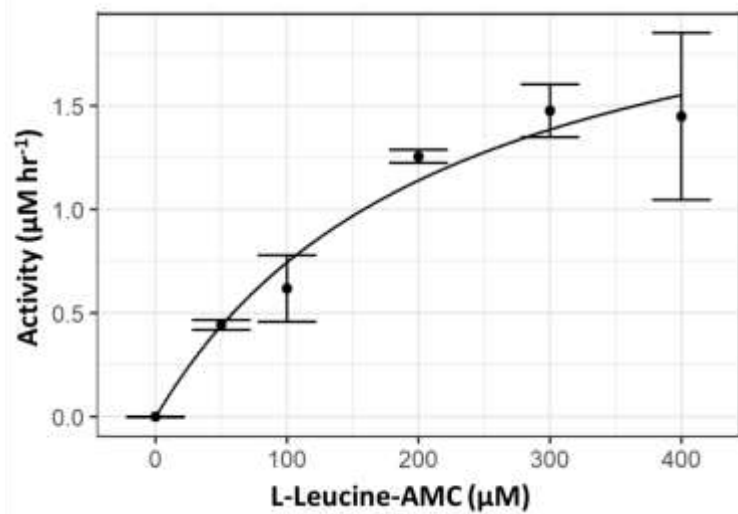
Figure II-2: Saturation curve of *S.* ACM-3962 acting on L-Leucine-AMC.

Presented are the average activities (points) and standard deviations (error bars) of three

replicates at each substrate concentration.
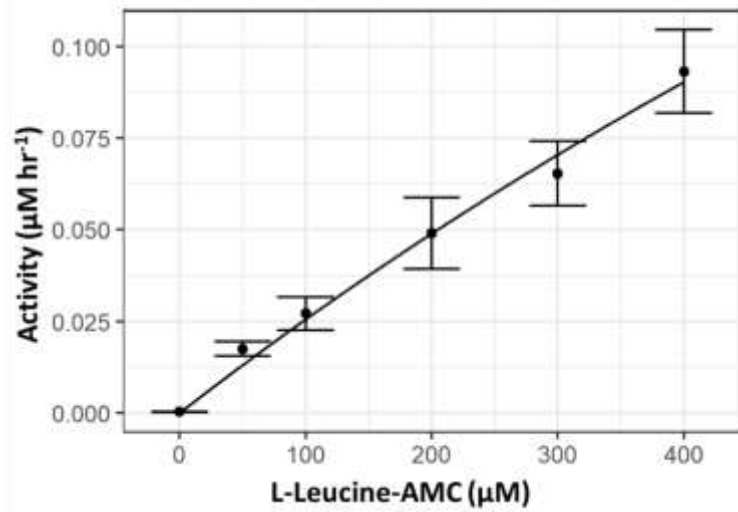
Figure II-3: Saturation curve of *E. coli* K12 acting on L-Leucine-AMC.

Presented are the average activities (points) and standard deviations (error bars) of three replicates at each substrate concentration. The activities here are an order of magnitude lower than the activities of the other two microbes.
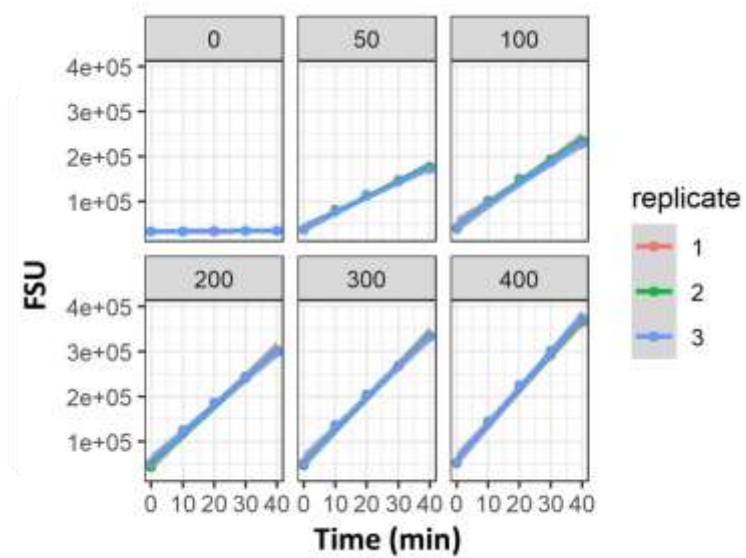
Figure II-4: Raw fluorescence data of *L. rhamnosus* GG acting on L-Leucine-AMC.

Faceted by substrate concentration (μM).
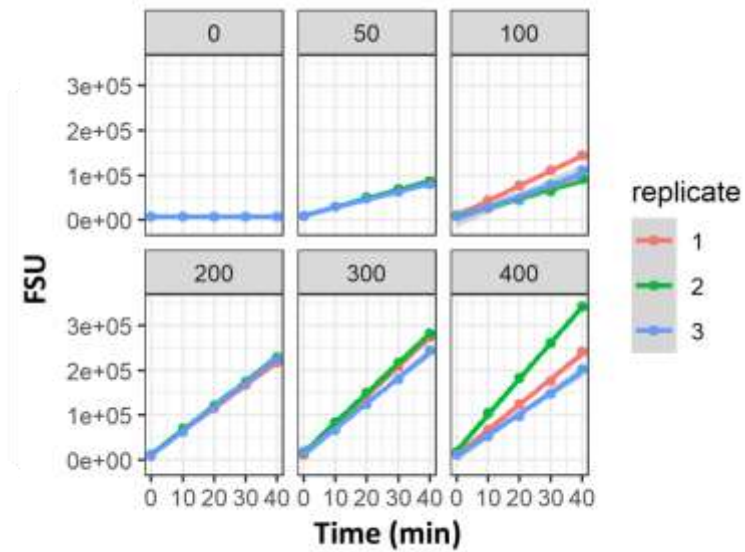
Figure II-5. Raw fluorescence data of *S.* ACM-3962 acting on L-Leucine-AMC.

Faceted by substrate concentration (μM).
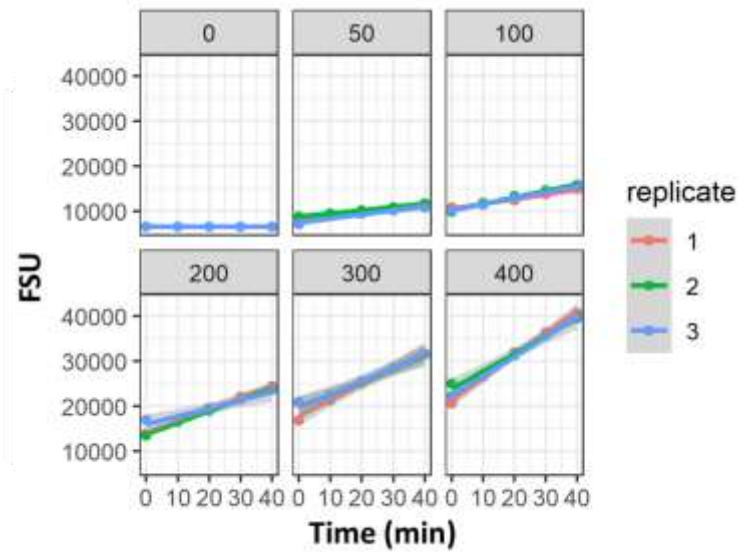
Figure II-6: Raw fluorescence data of *E. coli* K12 acting on L-Leucine-AMC.

Faceted by substrate concentration (µM).
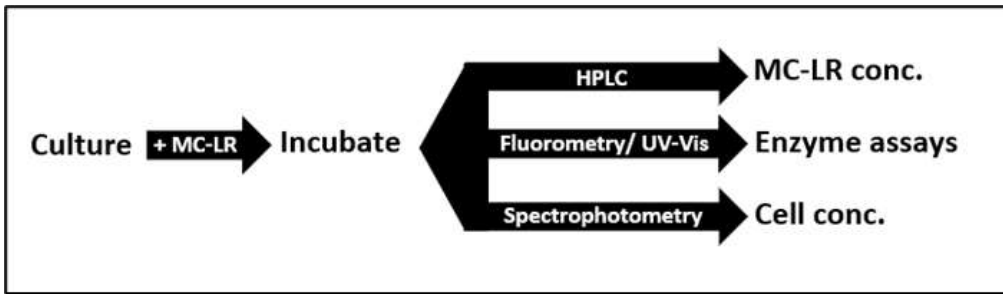
Figure II-7: Outline of future incubation experiments.

CHAPTER III
ezmmek: AN R PACKAGE TO ANALYZE EXTRACELLULAR ENZYME ACTIVITIES ON SYNTHETIC SUBSTRATES

Abstract

Extracellular enzyme assays are used to measure the enzyme activities of microbes toward complex organic matter. However, there are broad methodologies for assaying enzyme activities, and there remains a need to standardize the protocols used by practitioners. Here we describe *ezmmek* (Easy Michaelis-Menten Enzyme Kinetics), an R package designed to calculate enzyme kinetic parameters using published methodologies. *ezmmek* includes functions to calibrate, calculate, and plot enzyme activities as they relate to the transformation of synthetic substrates. At present, *ezmmek* implements two common protocols found in the literature, and is modular to accommodate additional protocols. Both common protocols were applied to the same freshwater samples prior to analysis in *ezmmek* and resulted in substantially different activities from identical data. We probe the reasons that the two methods yield different results from identical data and make recommendations as to which methods are appropriate for several sample types. As a reliable platform to compare and run different protocols, *ezmmek* aims to stimulate further discussion about how to best optimize extracellular enzyme assays.

Introduction

Optimization of Extracellular Enzyme Assays

Extracellular enzymes produced by microorganisms play an important role in driving ecosystem processes and biogeochemical cycles. Extracellular enzyme assays were developed as methods to quantify enzymatic activity and further probe the interactions between microbes and organic matter. Fluorometric assays, which involve

35

the detection of a fluorophore enzymatically cleaved from a substrate, are particularly popular due to their inexpensive, efficient, and accessible nature. The fluorescence of a sample ideally increases with respect to time, and can be converted to fluorophore production as a result of enzymatic hydrolysis. Although fluorometric assays are relatively simple in practice, several parameters can hinder the ability to measure activity values accurately. These parameters include 1) Adsorption of the fluorophore to solid surfaces, 2) Quenching of the fluorophore by dissolved compounds, 3) Abiotic release of the fluorophore from the substrate, and 4) Pre-existing background fluorescence (German et al., 2011).   Each of these parameters complicates the detection of fluorescence solely as a result of enzymatic hydrolysis. As an important step in describing a standardized approach to fluorometric enzyme assays, German et al. (2011) synthesize how best to correct for fluorometric interference by describing a protocol, complete with calculations and guidelines to address the effects of pH and temperature. However, the protocol described by German et al. (2011) has not been universally accepted among fluorometric assay practitioners. Other approaches differ in regard to how quenching is corrected and activity is calculated. The next step forward in creating a unified outlook on extracellular enzyme assay protocol is to compare other prominent protocols with the one described by German et al. (2011).

Protocol Descriptions

The protocol outlined by German et al. (2011), which will be referred to as the "In-Buffer Calibration (IBC) Protocol," corrects for quenching by measuring the interference from each individual component involved in an assay (Figure III-1;

Equations III-1 through III-4). The IBC Protocol involves standard curves in the separate

presence of homogenate (slurry of soil and buffer) and buffer. Also involved are

homogenate controls (i.e., sample slurry without added substrate), and substrate controls

(i.e., substrate in the presence of buffer without sample slurry). The separate standard

curves correct for quenching of the fluorophore in two different solutions, which can

affect later activity calculations. The homogenate and substrate controls correct for

background fluorescence and abiotic degradation of the substrate, respectively. The IBC

protocol measures activity based on one timepoint, which relies on the assumption that

fluorescence in the sample at time zero is equal to the fluorescence of the homogenate

control, corrected for quenching by the quench coefficient, minus the fluorescence of the

substrate control.

$$(\text{III-1}) \; V_{0,\text{Enzymes}} \; (\text{mol kg}^{-1} \, \text{s}^{-1}) = \frac{\text{Net Fluorescence (fsu)} * \text{Buffer Volume (L)}}{\text{Emission Coefficient} * \text{Homogenate Volume (L)} * \text{Time (s)} * \text{Soil Mass (kg)}}$$

$$(\text{III-2}) \; \text{Net Fluorescence (fsu)} = \frac{\text{Assay (fsu)} - \text{Homogenate Control (fsu)}}{\text{Quench Coefficient}} - \text{Substrate Control (fsu)}$$

$$(\text{III-3}) \; \text{Emission Coeff. (fsu mol}^{-1}) = \frac{\text{Slope of Standard Curve (in presence of homogenate)} \left[\frac{\text{fsu}}{\frac{\text{mol}}{\text{L}}}\right]}{\text{Standard Volume (L)}}$$

$$(\text{III-4}) \; \text{Quench Coeff.} = \frac{\text{Slope of Standard Curve (in presence of homogenate)} \left[\frac{\text{fsu}}{\frac{\text{mol}}{\text{L}}}\right]}{\text{Slope of Standard Curve (in presence of buffer)} \left[\frac{\text{fsu}}{\frac{\text{mol}}{\text{L}}}\right]}$$

As written, the IBC protocol only applies to samples with a solid component, such as soil

or sediment. To adjust this protocol for water samples, we replaced the soil mass from

Equation III-1 with the homogenate volume, as seen in Equation III-5. When a solid is

not present, the homogenate can simply be defined as the water sample in its entirety.

$$\text{(III-5) } V_{0,\text{Enzymes}} \text{ (mol L}^{-1} \text{ s}^{-1}) = \frac{\text{Net Fluorescence (fsu)} * \text{Buffer Volume (L)}}{\text{Emission Coefficient} * \text{Homogenate Volume (L)} * \text{Time (s)} * \text{Homogenate Volume (L)}}$$

Equations III-1 through III-5 were edited from German et al. (2011) to reflect the

International System (SI) of Units.

In contrast to the IBC Protocol, early environmental extracellular enzyme assays

simply measured the change in fluorescence per unit time of a live sample versus that

same rate of change of an autoclaved or killed sample (Hoppe, 1983; Somville & Billen,

1983; King, 1986), with a calibration curve measured using fluorophore added to the

sample. This protocol will be referred to as the "In-Sample Calibration (ISC) Protocol"

(Equations III-6 through III-9). In contrast to the widespread use of the IBC Protocol

within the soil microbial ecology community (DeForest, 2009; Allison et al., 2009; Stone

et al., 2012; Burns et al., 2013), the ISC Protocol has been widely used within the aquatic

microbial ecology community (Baltar et al., 2009; Baltar et al., 2010; Steen & Arnosti,

2011). The ISC Protocol corrects for quenching by measuring "bulk" interference, which

relies on the assumption that the behavior of the free fluorophore released from substrates

behaves identically to the free fluorophore added to the sample to construct a calibration

curve. Some workers have modified the ISC Protocol to account for potential sorption of

fluorophore to particles over the time course of the incubation (Coolen & Overmann,

2000). This is relevant in samples with very high organic content, e.g., marine sapropels,

but does not appear to be relevant in typical marine sediments (Steen et al., 2019). This

can be corrected by applying a separate calibration curve at each timepoint, but we do not address it here.

The ISC Protocol uses a standard curve in the presence of homogenate-buffer solution and killed controls, which comprise of substrate in the presence of autoclaved or boiled homogenate-buffer solution; Figure III-1). Activity is calculated as the slope (m_{fl}) of concentration of fluorophore (mol L^{-1}; after conversion from fluorescence units) with respect to time (s), which requires a minimum of two timepoints.

$$(\text{III-6}) \; V_{0,\text{Enzymes}} \, (\text{mol kg}^{-1} \, \text{s}^{-1}) =$$

$$V_{0,\text{Sample}} \, (\text{mol kg}^{-1} \, \text{s}^{-1}) - V_{0,\text{Killed Control}} \, (\text{mol kg}^{-1} \, \text{s}^{-1})$$

Activity for either the sample or the killed control is calculated as:

$$(\text{III-7}) \; V_0 = \frac{m_{fl} \; (\text{mol L}^{-1}\text{s}^{-1})}{\text{Soil Mass (kg)}} * \text{Assay Volume (L)}$$

$$(\text{III-8}) \; \text{Fluorophore} \, (\text{mol L}^{-1}) =$$

$$\frac{\text{Fluorescence (fsu)} - \; \text{Intercept of Standard Curve (in presence of homogenate and buffer solution) [fsu]}}{\text{Slope of Standard Curve (in presence of homogenate and buffer solution)} \left[\frac{\text{fsu}}{\frac{\text{mol}}{\text{L}}}\right]}$$

For a liquid sample or killed control, Equation III-7 can be simplified as follows:

$$(\text{III-9}) \; V_0 \, (\text{mol L}^{-1} \, \text{s}^{-1}) = \; m_{fl} \; (\text{mol L}^{-1}\text{s}^{-1})$$

Methods

Design of ezmmek

ezmmek (Easy Michaelis-Menten Enzyme Kinetics) is a package designed for R, an open source statistical software environment becoming increasingly useful in the

fields of ecology and other biological sciences. The most current iteration of *ezmmek* (v. 0.2.0) can be found on GitHub (https://github.com/ccook/ezmmek). Using S3 object-oriented programming, *ezmmek* contains a suite of functions that output relevant analyses as data frames belonging to unique *ezmmek* classes (Table III-1). The user can further analyze these data frame objects using generic R functions, such as *plot*, that were assigned new methods to process these new classes.

ezmmek operates under a hierarchal structure, in that the data frame output of each function builds upon the data frame output of a lower-tier function (Table III-1). For example, the data frame created by *new_ezmmek_sat_fit* includes standard curve data and analyses that build on that standard curve data. But if the user only wishes to analyze standard curve data, then they can run the more appropriate *new_ezmmek_std_curve*. The workflow of *ezmmek* treats the standard curve data and raw activity data as separate files that are analyzed independent from each other before being combined for more complex analyses (Figure III-2). During this flow, the user must specify which protocol they are using to determine how final activity is calculated. Code for each *ezmmek* function can be found in the appendix.

Sample and Site Description

A freshwater sample was collected at approximately 10:00 AM from Third Creek in Tyson Park (2351 Kingston Pike, Knoxville, TN 37919), under the walking bridge near the intersection of South Concord Street and Tyson McGhee Park Street Southwest (Figure III-3). Conditions were sunny, with a temperature of approximately 13 °C.

Enzyme assays using both protocols were performed as soon as possible once samples were transported to the laboratory later that morning.

Enzyme Assay Procedure

Enzyme assay parameters should be adjusted to match the environmental conditions of the sample site. As this study primarily focuses on the effect of the protocol, the effects of these other parameters, such as pH and temperature, were deemed inessential, as long as reasonable saturating conditions were observed. Here, the buffer used was phosphate-buffered saline (PBS), and the homogenate used was the freshwater sample. The pHs of the buffer and homogenate were 7.27 and 8.04, respectively. The experiment was performed at ambient temperature. pH and temperature were assumed equal and constant for both protocols for the duration of the experiment. Enzyme assays were performed using L-Leucine-AMC, a fluorogenic substrate that serves as an analog for the environmentally common and highly digestible amino acid, L-Leucine.

Standard curves were measured in the presence of homogenate, buffer, and homogenate-buffer solution. The standard curve aliquots were made in 1.5 mL plastic cuvettes and measured using a Promega^{TM} GloMax$^{®}$ fluorometer. For the standard curve in the separate presence of homogenate and buffer (IBC Protocol), each aliquot consisted of 960 µL of homogenate or buffer, and 40 µL of a varying ratio of dimethyl sulfoxide (DMSO) to AMC dissolved in DMSO, with the ratio dependent on the desired concentration of AMC in the final solution. For the standard curve in the presence of homogenate-buffer solution (ISC Protocol), each aliquot consisted of 860 µL of homogenate, 100 µL of buffer, and 40 µL of a varying ratio of dimethyl sulfoxide

(DMSO) to AMC dissolved in DMSO, with the ratio dependent on the desired concentration of AMC in the final solution. Under both protocols, final concentrations of AMC were 0.0, 1.0, 2.0, 3.0, and 4.0 µM. Aliquots were made in duplicate for each of the standard curves. These data were saved in long-format as a comma-separated values (CSV) file for analysis in *ezmmek*.

Raw fluorescence data were measured in the presence of homogenate-buffer solution at time intervals of 0, 20, 40, 60, 120, and 240 minutes. For the ISC Protocol, each of these timepoints were used to calculate activities. For the IBC Protocol, which relies on a single timepoint, only data collected at the 240-minute mark was used to calculate activities. These aliquots were prepared in similar fashion to the homogenate-buffer solution standard curve aliquots, with each cuvette consisting of 860 µL of homogenate, 100 µL of buffer, and a 40 µL ratio of DMSO and L-Leucine-AMC dissolved in DMSO. Final solution L-Leucine-AMC substrate concentrations, which were prepared in triplicate, were 0, 50, 100, and 200 µM. Following the ISC Protocol, this same process was repeated, but with the killed control taking place of the homogenate. For the IBC Protocol, the substrate control took place of the homogenate. Data relevant to both the ISC and IBC were saved in separate long-format comma-separated values (CSV) files. Both sets of data were analyzed in *ezmmek*. The buffer volume, as seen in Equation III-5, was considered to be the summation of PBS volume and DMSO volume, which was 140 µL.

Results and Discussion

ezmmek Performance

ezmmek successfully analyzed several aspects of extracellular enzyme data, including enzyme kinetic parameters, data visualizations, and relevant statistics. However, some useful features are still in development. These include the ability to 1) Input and track units throughout the analyses and 2) Read in different file formats of data.

Enzyme Assay Method Analysis

The standard curve, raw data, and saturation curve plots produced by ezmmek can be found in this chapter's appendix. Final average V_0 calculations between the two protocols differed by a maximum of two orders of magnitude (Table III-2). At 200 µM L-Leucine-AMC, the maximum substrate concentration at which activity was measured, the IBC Protocol calculated an average V_0 of 0.845 nM hr^{-1} (Figure III-11), and the ISC Protocol calculated an average V_0 of 85.1 nM hr^{-1} (Figure III-12). The difference in final average activities can be traced to the calculation method of each protocol, particularly in regard to the number of timepoints collected. By collecting a single timepoint, the IBC Protocol assumes that fluorescence units (fsu) at time zero, after accounting for the fsu values of the controls, equal zero. In this study, this assumption did not hold true. The error bar associated with average activity at 200 µM L-Leucine AMC, as determined by the IBC Protocol, was large compared to the error bars corresponding to the other substrate concentrations, with half of it covering a negative range of activities (Figure III-11). The sample fluorescence values of Replicates 1, 2, and 3 at Time 120 minutes were

143328.50, 83360.85, and 140409.87 fsu, respectively. The corresponding substrate

control fluorescence values of these replicates were 68130.94, 73493.61, and 58215.49,

respectively. The substrate control values were less spread than the sample values.

Because each of the sample values were assumed to have the same starting fsu value of

zero, replicate 2 was calculated to have less activity than the other two replicates. The

activity calculations for replicate 2 at substrate concentration 200 µM rely on the IBC

Protocol equations discussed previously and are as follows:

$$\text{Emission Coefficient } = \frac{404 * \left[\frac{\frac{fsu}{nmol}}{L}\right]}{1 * 10^{-3} \text{ L}} = \mathbf{4.05 * 10^5 \text{ fsu nmol}^{-1}}$$

$$\text{Quench Coefficient} = \frac{404 \left[\frac{\frac{fsu}{nmol}}{L}\right]}{235 \left[\frac{\frac{fsu}{nmol}}{L}\right]} = \mathbf{1.72}$$

$$\text{Net Fluorescence} = \frac{8.32 * 10^4 \text{ fsu} - 1.38 * 10^3 \text{ fsu}}{1.72} - 7.3 * 10^4 \text{ fsu} = \mathbf{-2.60 * 10^4 \text{ fsu}}$$

$$\text{Activity } = \frac{-2.60*10^4 \text{ fsu} * 1.4 * 10^{-4} \text{ L}}{4.05*10^5 \text{ fsu nmol}^{-1} * 8.6 * 10^{-4} \text{ L} * 2 \text{ h} * 8.6 * 10^{-4} \text{ L}} = \textbf{-6.08 nM h}^{\textbf{-1}}$$

Note that these calculations were rounded for ease of reading. Due to the negative net

fluorescence value, which comes from the fact that fluorescence of replicate 2's control

was greater than the fluorescence at the initial timepoint of the sample, the IBC Protocol

calculated the activity of replicate 2 as a negative value. Replicate 2 was primarily

responsible for the large amount of error at 200 µM L-Leucine-AMC. However, the raw

fluorescence data collected by the ISC Protocol, which shows change in fsu with respect

to time (Figure III-10), suggested that the activities of these three replicates at 200 µM

were closer in value than calculated by the IBC Protocol. Replicate 2 appeared to be

offset from the other replicates, but maintained a similar slope, which implied a positive

activity value. The substrate control for replicate 2, however, did not appear to be offset (Figure III-9). The following activity calculations for replicate 2 at substrate concentration 200 µM relied on the ISC Protocol equations discussed previously and are as follows:

$$\text{Sample Fluorophore after 2 h} = \frac{8.32 * 10^4 \text{ fsu} - 1.24 * 10^4 \text{ fsu}}{2.68 * 10^2 \left[\frac{\text{fsu}}{\frac{\text{nmol}}{\text{L}}}\right]} = \textbf{355 nM}$$

$$\text{Sample Fluorophore after 0 h} = \frac{8.40 * 10^4 \text{ fsu} - 1.24 * 10^4 \text{ fsu}}{2.68 * 10^2 \left[\frac{\text{fsu}}{\frac{\text{nmol}}{\text{L}}}\right]} = \textbf{77.3 nM}$$

$$V_{0, \text{ Sample}} = \frac{355 \text{ nM} - 77.3 \text{ nM}}{2 \text{ h} - 0 \text{ h}} = \textbf{139 nM h}^{\textbf{-1}}$$

$$\text{Killed Control Fluorophore after 2 h} = \frac{9.75 * 10^4 \text{ fsu} - 12.4 * 10^4 \text{ fsu}}{269 \left[\frac{\text{fsu}}{\frac{\text{nmol}}{\text{L}}}\right]} = \textbf{409 nM}$$

$$\text{Killed Control Fluorophore after 0 h} = \frac{5.96 * 10^4 \text{ fsu} - 12.4 * 10^4 \text{ fsu}}{269 \left[\frac{\text{fsu}}{\frac{\text{nmol}}{\text{L}}}\right]} = \textbf{268 nM}$$

$$V_{0, \text{ Killed Control}} = \frac{409 \text{ nM} - 268 \text{ nM}}{2 \text{ h} - 0 \text{ h}} = \textbf{71.3 nM h}^{\textbf{-1}}$$

$$V_{0, \text{ Enzymes}} = V_{0, \text{ Sample}} - V_{0, \text{ Killed Control}} = \textbf{67.7 nM h}^{\textbf{-1}}$$

Note that this simplified and rounded version only relied on the first and last timepoint to calculate activity. Normally, the slope would be calculated from a line of multiple timepoints.

The enzymatic activities of each replicate at 200 µM L-Leucine-AMC, in addition to their corresponding averages and standard deviations, are shown in Table III-2. Positive activities were calculated for both the sample and the killed control of replicate 2. The concentration of fluorophore was greater at both timepoints for the killed control than the sample. However, this observation is largely irrelevant, as the ISC Protocol

considers only the rate of change between them, which in this instance was greater for the sample activity. Even though the killed control values were higher than the sample values, they increased in fsu over time at a lesser rate than the assay values, resulting in a positive rate of change between timepoints (Figures III-10 and III-11). The IBC Protocol does not account for any potential offsets with its substrate control and will always result in a negative activity if the fsu of the substrate control is greater than the fsu of the assay. The lack of accounting for potential offsets may also explain why the IBC calculated substantially lower activities in this instance. The ISC Protocol appeared to be less sensitive to offsets between replicates and potential pipetting errors than the IBC Protocol by taking multiple timepoints. The IBC Protocol may benefit by taking multiple timepoints, if only as a check to ensure that the zero-fsu at time zero assumption holds true. The mechanisms behind the offsets in this study are unclear, but they may be related to naturally fluorescent organics heterogeneously distributed in the sample.

Conclusions

ezmmek is a useful tool for analyzing several aspects of enzyme assay data and will hopefully spur more conversation about how to best optimize environmental extracellular enzyme assays. The IBC Protocol appears to be more sensitive to offsets between replicates than the ISC Protocol. In an experiment where the difference in release of fluorophore due to abiotic mechanisms versus enzymatic hydrolysis is small, the ISC Protocol may be better suited to measure those activities. However, some studies suggest that autoclaving or boiling the homogenate does not fully deactivate enzymes (Carter et al., 2007). A killed control could then overcalculate the amount of abiotic

release of fluorophore from the substrate, which in turn would cause an undercalculation of enzymatic activity. More robust comparisons, particularly for soil and sediment samples, need to be performed before further assessing the strengths and weaknesses of each protocol.

References

Allison, S.D., LeBauer, D.S., Ofrecio, M.R., Reyes, R., Anh-Minh, Ta, & Tran, T.M. (2009). Low levels of nitrogen addition stimulate decomposition by boreal forest fungi. *Soil Biology and Biochemistry*, *41*(2), 293-302.

Baltar, F., Arístegui, J., Sintes, E., Van Aken, H.M., Gasol, J.M., & Herndl, G.J. (2009). Prokaryotic extracellular enzymatic activity in relation to biomass production and respiration in the meso- and bathypelagic waters of the (sub)tropical Atlantic. *Environmental Microbiology, 11*(8), 1998-2014.

Baltar, F., Arístegui, J., Gasol, J.M., Sintes, E., Van Aken, H.M., & Herndl, G.J. (2010). High dissolved extracellular enzymatic activity in the deep central Atlantic Ocean. *Aquatic Microbial Ecology, 58*(3), 287-302.

Burns, R.G., DeForest, J.L., Marxsen, J., Sinsabaugh, R.L., Stromberger, M.E., Wallenstein, M.D., Weintraub, M.N., & Zoppini, A. (2013). Soil enzymes in a changing environment: Current knowledge and future directions. *Soil Biology and Biochemistry*, *58*, 216-234.

Carter, D.O., Yellowlees, D., & Tibbett, M. (2007). Autoclaving kills soil microbes yet soil enzymes remain active. *Pedobiologia, 51*, 295-299.

Coolen, M.L.J. & Overmann, J. (2000). Functional exoenzymes as indicators of metabolically active bacteria in 124,000-year-old sapropel layers of the eastern Meditteranean Sea. *Applied Environmental Microbiology, 66*(6), 2589-2598.

DeForest, J.L. (2009). The influence of time, storage temperature, and substrate age on potential soil enzyme activity in acidic forest soils using MUB-linked substrates and L-DOPA. *Soil Biology and Biochemistry*, *41*(6), 1180-1186.

German, D.P., Weintraub, M.N., Grandy, A.S., Lauber, C.L., Rinkes, Z.L., & Allison,

    S.D. (2011). Optimization of hydrolytic and oxidative enzyme methods for

    ecosystem studies. *Soil Biology and Biochemistry*, *43*(7), 1387–1397.

Hoppe, H. (1983). Significance of exoenzymatic activities in the ecology of brackish

    water: Measurements by means of methylumbelliferyl-substrates. *Marine Ecology*

    Progress Series, *11*, 299-308.

King, G.M. (1986). Characterization of β-glucosidase activity in intertidal marine

    sediments. *Applied and Environmental Microbiology, 50*(3), 231-237.

Somville, M. & Billen, G. (1983). A method for determining exoproteolytic activity in

    natural waters. *Limnology and Oceanography, 28*(1), 190-193.

Steen, A.D. & Arnosti, C. (2011). Long lifetimes of β-glucosidase, leucine

    aminopeptidase, and phosphatase in Arctic seawater. *Marine Chemistry, 123*, 127-

    132.

Steen, A.D., Kevorkian, R.T., Bird, J.T., Dombrowski, N., Baker, B.J., Hagen, S.M.,

    Mulligan, K.H., Schmidt, J.M., Webber, A.T, Royalty, T.M., & Alperin, M.J. (2019).

    Kinetics and identities of extracellular peptidases in subsurface sediments of the

    White Oak River Estuary, North Carolina. *Environmental Microbiology, 85*(19), 102-

    119.

Stone, M.M, Weiss, M.S., Goodale, C.L., Adams, M.B., Fernandez, I.J., German, D.P.,

    and Allison, S.D. (2012). Temperature sensitivity of soil enzyme kinetics under N-

    fertilization in two temperate forests. *Global Change Biology, 18*(3), 1173-1184.

Appendix

Table III-1: Descriptions of *ezmmek* functions.

Functions that begin with "*new*" are those that create objects of a new class and are accessible to the user. These "*new*" functions are listed in descending order by tier, with *new_ezmmek_sat_fit* being of the highest tier and building upon those functions listed below it. Functions that begin with "*ezmmek*" perform calculations and are inaccessible to the user.

Function/ Class of New Data Frame	Output/ Purpose	User Access
new_ezmmek_sat_fit	Tibble containing predicted saturation curve	Exported
new_ezmmek_act_calibrate	Tibble containing calibrated activity data	Exported
new_ezmmek_act_group	Tibble containing grouped raw activity data	Exported
new_ezmmek_std_group	Tibble containing grouped raw standard curve data	Exported
ezmmek_calc_mm_fit	Calculates Michaelis-Menten fit	Hidden
ezmmek_calibrate_activities	Calibrates raw activity data by standard curve	Hidden
ezmmek_std_lm	Applies predicted standard curve models to nested datasets	Hidden
ezmmek_calc_std_buffer	Calculates standard curve in presence of buffer	Hidden
ezmmek_calc_std_homo	Calculates standard curve in presence of homogenate	Hidden

Table III-2: Enzymatic activities and their corresponding averages and standard deviations of each replicate at 200 μM substrate under both protocols.

Protocol	Replicate	V_0 (activity; nM h^{-1})	Average V_0	Standard Deviation
IBC	1	3.35		
	2	-6.08	0.845	6.07
	3	5.28		
ISC	1	112		
	2	71.3	85.1	23.7
	3	71.6		

Figure III-1: Standards and controls used for each protocol.

Both protocols use the same assay sample, but calculate activity based on different standards, controls, and equations.
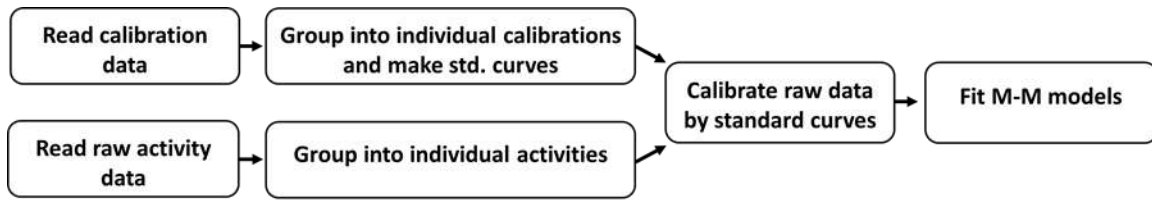
Figure III-2: *ezmmek* **design flow.**

Standard curve data and raw activity data are read as separate files before being

processed to calculate final activity data and fit Michaelis-Menten models. Michaelis-

Menten models include the kinetics parameters of K_M and V_{Max}.

Figure III-3: Sampling location at Tyson Park, Knoxville, TN 37919.

The sampling location is marked with a red box under the aerial view (A), which marks

the approximate location of the street view (B).
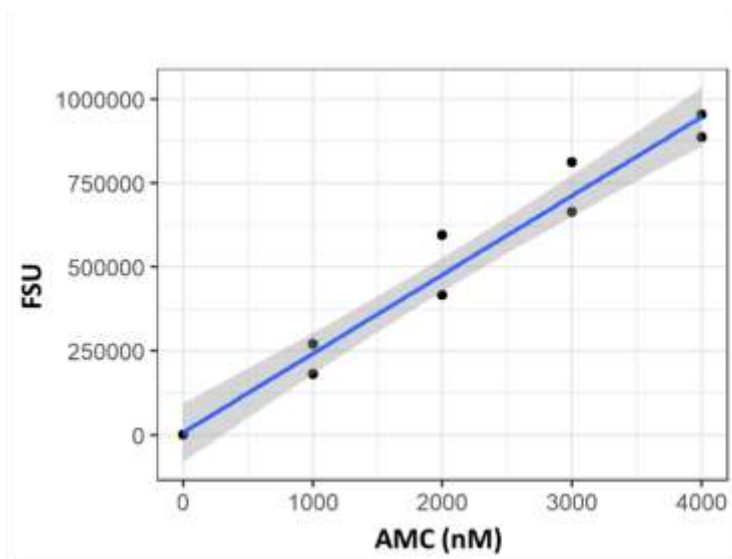
```
## Call:
## lm(formula = buffer_signal ~ std_conc, data = gcal$std_raw_data_g[[1
]])
##
## Residuals:
##    Min     1Q Median     3Q    Max
## -61817 -58412  -7289  21906 117357
##
## Coefficients:
##              Estimate Std. Error t value Pr(>|t|)
## (Intercept) 7771.83    37845.24   0.205    0.842
## std_conc     235.10       15.45  15.216 3.45e-07 ***
## ---
## Signif. codes:  0 '***' 0.001 '**' 0.01 '*' 0.05 '.' 0.1 ' ' 1
##
## Residual standard error: 69100 on 8 degrees of freedom
## Multiple R-squared:  0.9666, Adjusted R-squared:  0.9624
## F-statistic: 231.5 on 1 and 8 DF,  p-value: 3.448e-07
```

Figure III-4: Standard curve in buffer and model summary statistics, IBC Protocol.
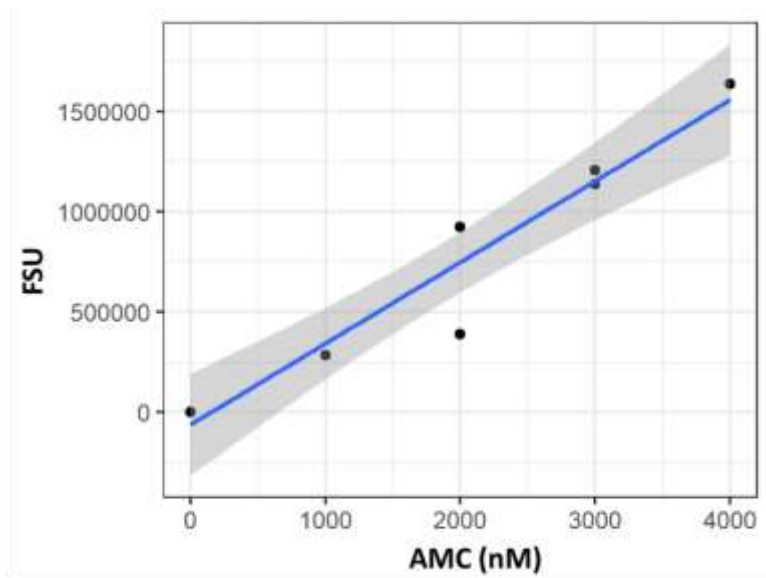
```
## Call:
## lm(formula = homo_signal ~ std_conc, data = gcal$std_raw_data_g[[1]]
)
##
## Residuals:
##     Min      1Q  Median      3Q     Max
## -358024  -26326   57618   66902  175999
##
## Coefficients:
##              Estimate Std. Error t value Pr(>|t|)
## (Intercept) -61510.19  104029.08  -0.591 0.575916
## std_conc       404.78      44.87   9.021 0.000104 ***
## ---
## Signif. codes:  0 '***' 0.001 '**' 0.01 '*' 0.05 '.' 0.1 ' ' 1
##
## Residual standard error: 173100 on 6 degrees of freedom
##   (2 observations deleted due to missingness)
## Multiple R-squared:  0.9313, Adjusted R-squared:  0.9199
## F-statistic: 81.38 on 1 and 6 DF,  p-value: 0.0001039
```

Figure III-5: Standard curve in homogenate and model summary statistics, IBC Protocol.

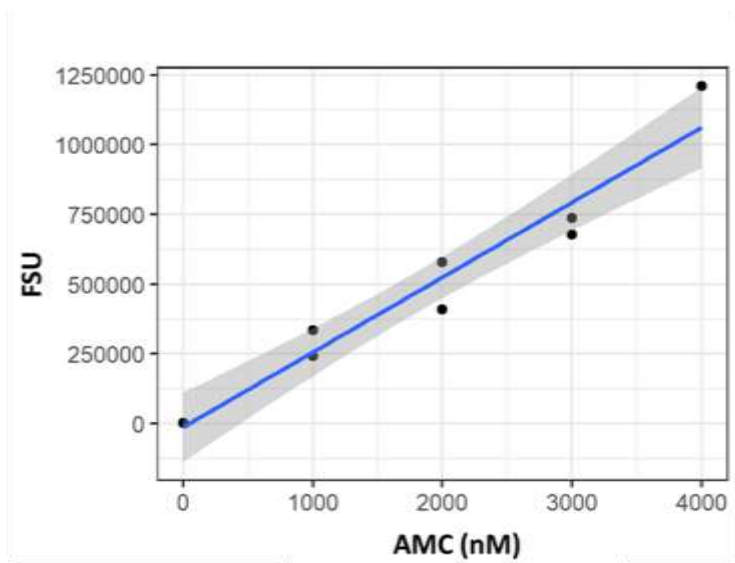```
Call:
lm(formula = homo_buffer_signal ~ std_conc, data = ssat$std_raw_data
_s[[1]])
##
Residuals:
Min   1Q Median   3Q   Max
-117425 -56536   13777   53831 146012
##
Coefficients:
Estimate Std. Error t value Pr(>|t|)
(Intercept) -12363.58   52455.51 -0.236   0.82
std_conc   268.71   23.72 11.327 9.36e-06 ***

Signif. codes: 0 '***' 0.001 '**' 0.01 '*' 0.05 '.' 0.1 ' ' 1
##
Residual standard error: 93570 on 7 degrees of freedom
(1 observation deleted due to missingness)
Multiple R-squared: 0.9483, Adjusted R-squared: 0.9409
F-statistic: 128.3 on 1 and 7 DF, p-value: 9.36e-06
```

**Figure III-6: Standard Curve in homogenate-buffer solution and model summary statistics, ISC Protocol.**
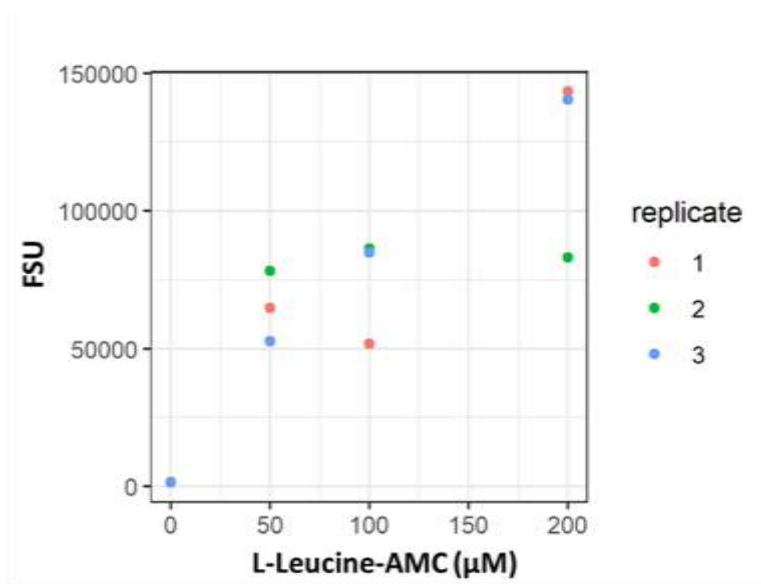
**Figure III-7: Raw fluorescence data, IBC Protocol.**

Generated using *new_ezmmek_act_group.* Data was collected at time 120 minutes.
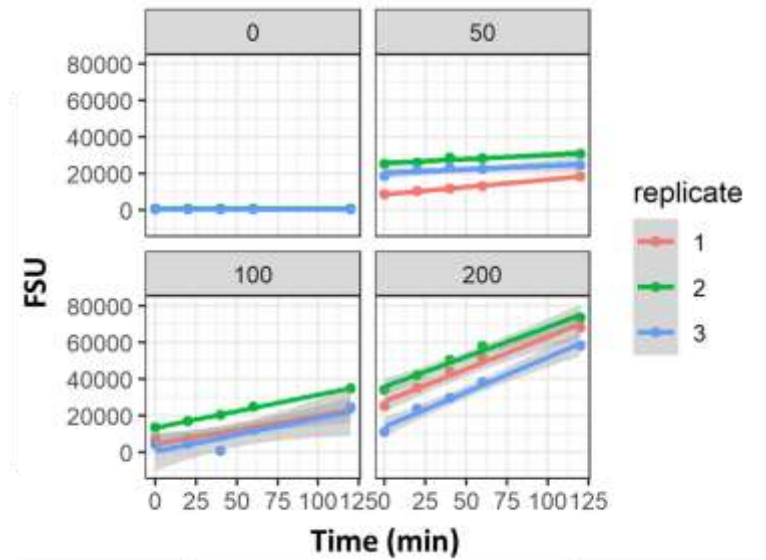
**Figure III-8: Raw substrate control data, IBC Protocol.**

Faceted by substrate concentration (µM). The IBC Protocol typically relies on one

timepoint, but the timepoints here were collected in tandem with the ISC Protocol, which

relies on taking several timepoints.
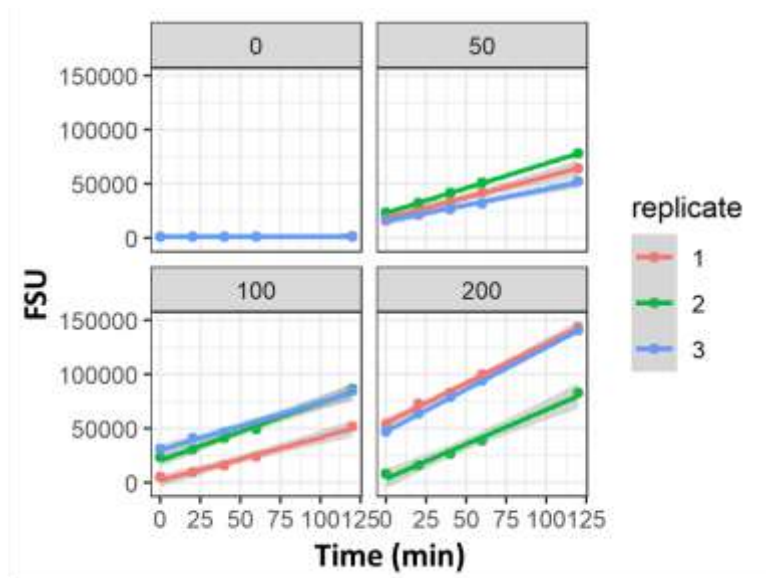
**Figure III-9: Raw fluorescence data, ISC Protocol.**

Generated using *new_ezmmek_act_group*. Faceted by substrate concentration (µM).
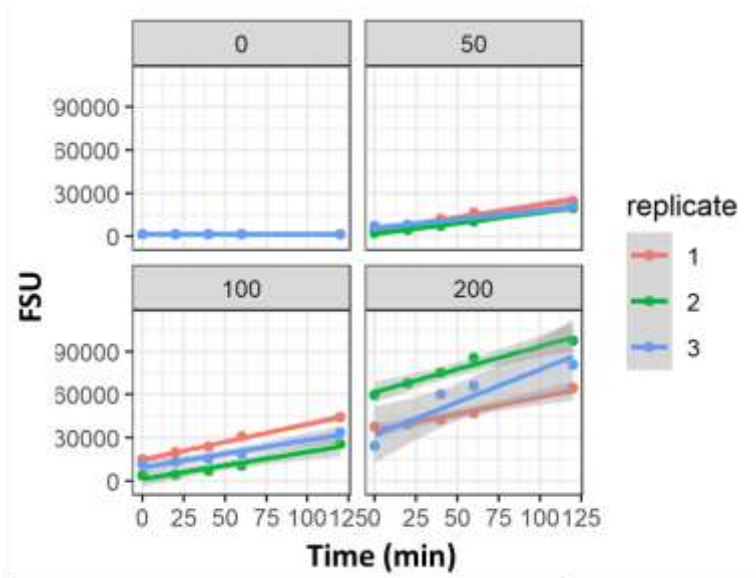
**Figure III-10: Raw killed control data, ISC Protocol.**

Faceted by substrate concentration (µM).
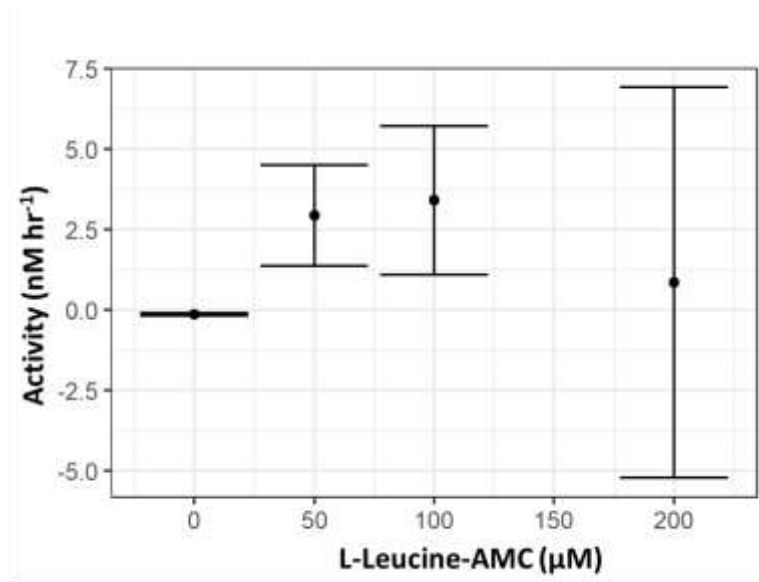
**Figure III-11: Calibrated activity data, IBC Protocol.**

Presented are the average activities (points) and standard deviations (error bars) of three
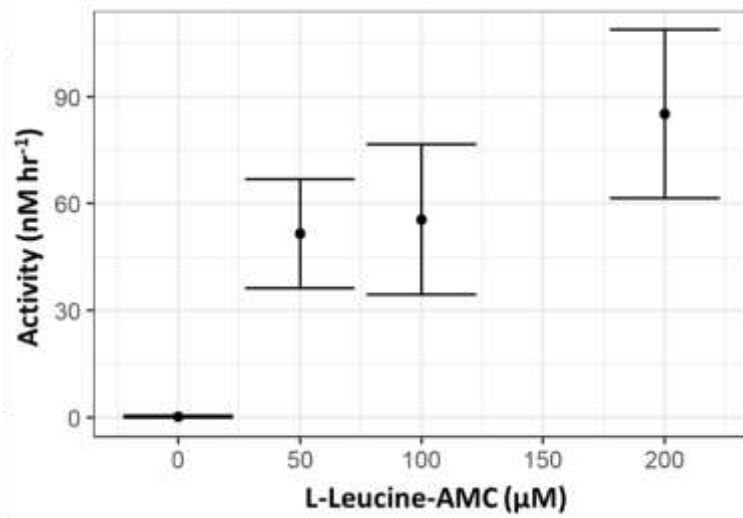
replicates.

**Figure III-12: Calibrated activity data, ISC Protocol.**

Presented are the average activities (points) and standard deviations (error bars) of three

replicates.
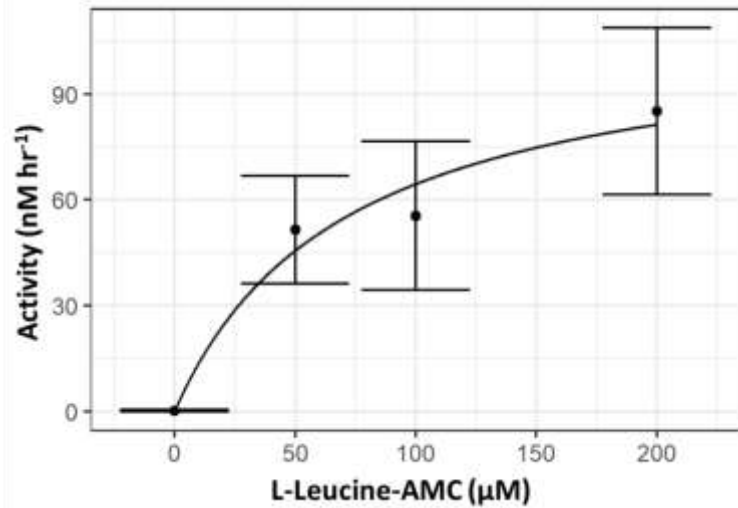
```
## Formula: activity_m ~ (vmax * substrate_conc)/(km + substrate_conc)
##
## Parameters:
##        Estimate Std. Error t value Pr(>|t|)
## vmax   110.172       4.670  23.593  < 2e-16 ***
## km      70.873       7.849   9.029 1.19e-12 ***
## ---
## Signif. codes:  0 '***' 0.001 '**' 0.01 '*' 0.05 '.' 0.1 ' ' 1
##
## Residual standard error: 5.798 on 58 degrees of freedom
##
## Number of iterations to convergence: 5
## Achieved convergence tolerance: 5.966e-06
```

Figure III-13: Saturation curve data and model summary statistics, ISC Protocol.

Presented are the average activities (points) and standard deviations (error bars) of three

replicates. A nonlinear model based on Michaelis-Menten kinetics was fitted to these

points.

Function III-1: *new_ezmmek_sat_fit*

```r
########
### Calculate Michaelis-Menten fit and add to dataframe
########


new_ezmmek_sat_fit <- function(std.data.fn,

                               act.data.fn,

                               ...,

                               km = NULL,

                               vmax = NULL,

                               method = NA) {


  ### User names columns to be grouped
  columns <- purrr::map_chr(rlang::enquos(...), rlang::quo_name)


  ### Calibrate and calculate activities
  calibrated_df <- new_ezmmek_act_calibrate(std.data.fn,

                                            act.data.fn,

                                            ...,

                                            method = method,

                                            columns = columns)


  ### Group data frame by substrate type and the additional arguments p
ut in by user
  calibrated_df_grouped <- calibrated_df %>%

    dplyr::group_by_at(dplyr::vars(substrate_type, intersect(names(.),
columns))) %>%

    tidyr::nest()


  ### Creates new Michaelis-Menten fit columns
  calibrated_df_mm_fit <- calibrated_df_grouped %>%

    dplyr::mutate(mm_fit_obj = purrr::map(data, function(df) ezmmek_cal
c_mm_fit(df, km, vmax) %>% purrr::pluck(1)), #nlsm
```

```r
                  km = purrr::map_dbl(data, function(df) coef(ezmmek_ca
lc_mm_fit(df, km, vmax) %>% purrr::pluck(1))[2]), #km

                  vmax = purrr::map_dbl(data, function(df) coef(ezmmek_
calc_mm_fit(df, km, vmax) %>% purrr::pluck(1))[1]), #vmax

                  pred_grid = purrr::map(data, function(df) ezmmek_calc
_mm_fit(df, km, vmax) %>% purrr::pluck(2))) %>%

    tidyr::unnest(data)


  ### Function to apply mm_fit to each value in pred_grid

  predict_df <- function(mm_fit, pred_grid) {

    pred.vec <- predict(mm_fit, pred_grid)

    pred_df <- data.frame(substrate_conc = pred_grid$substrate_conc, ac
tivity_m = pred.vec)

    pred_df

  }


  ### Apply predict_df() to pred_grid in each row

  result_df <- calibrated_df_mm_fit %>%

    dplyr::mutate(pred_activities = purrr::map2(.x = mm_fit_obj, .y = p
red_grid, .f = predict_df))


  ### Assign new class

  class(result_df) <- c("new_ezmmek_sat_fit", "data.frame")


  result_df

}
```

Function III-2: *new_ezmmek_act_calibrate*

```r
########
### Join activity dataframe with standard dataframe and calibrate
########


new_ezmmek_act_calibrate <- function(std.data.fn,
                                     act.data.fn,
                                     ...,
                                     method = NA,
                                     columns = NULL) {


  ### Use '...' arguments if column names not supplied in parent fxn
  if(is.null(columns)) {
    columns <- purrr::map_chr(rlang::enquos(...), rlang::quo_name)
  }
  ### Creates dataframe of standard curve data
  std_data_grouped <- new_ezmmek_std_group(std.data.fn,
                                           method = method,
                                           columns = columns)


  ### Creates dataframe of raw activity data
  act_data_grouped <- new_ezmmek_act_group(act.data.fn,
                                           method = method,
                                           columns = columns)


  ### Joins the two data frames based on common descriptor columns
  std_act_std <- dplyr::full_join(act_data_grouped, std_data_grouped)


  ### Calibrate activities
  std_act_calibrated <- ezmmek_calibrate_activities(std_act_std, method
, columns)
```

```r
  ### Assign new class
  class(std_act_calibrated) <- c("new_ezmmek_calibrate", "data.frame")


  std_act_calibrated


}
```

Function III-3: *new_ezmmek_act_group*

```r
########
### Group raw activity data
########


new_ezmmek_act_group <- function(act.data.fn,
                                 ...,
                                 method = NA,
                                 columns = NULL) {


  ### Read in data
  act_data <- read.csv(act.data.fn)


  ### Use '...' arguments if column names not supplied in parent fxn
  if(is.null(columns)) {

    columns <- purrr::map_chr(rlang::enquos(...), rlang::quo_name)

  }


  ### Steen method required column names
  if(method == "steen") {

    assertable::assert_colnames(data = act_data,
                   colnames = c("time",
                                "signal",
                                "substrate_conc"),
                   only_colnames = FALSE,
                   quiet = TRUE)



  act_data_grouped <- act_data %>%
    dplyr::group_by_at(dplyr::vars(intersect(names(.), columns))) %>%
    dplyr::group_nest(.key = "act_raw_data_s")

  }
```

```r
  if(method == "german") {

    assertable::assert_colnames(data = act_data,
                    colnames = c("time",
                                 "signal",
                                 "substrate_conc",
                                 "buffer_vol",
                                 "homo_vol",
                                 "soil_mass",
                                 "assay_vol",
                                 "homo_control",
                                 "substrate_control"),
                    only_colnames = FALSE,
                    quiet = TRUE)


    act_data_grouped <- act_data %>%
      dplyr::group_by_at(dplyr::vars(intersect(names(.), columns))) %>%
      dplyr::group_nest(.key = "act_raw_data_g")
  }


  class(act_data_grouped) <- c("new_ezmmek_act_group", "data.frame")


  act_data_grouped


}
```

Function III-4: *new_ezmmek_std_group*

```r
########
### Group standard lm objects
########


new_ezmmek_std_group <- function(std.data.fn,

                                 ...,

                                 method = NA,

                                 columns = NULL) {


  ### Read in data
  std_data <- read.csv(std.data.fn)


  ### Use '...' arguments if column names not supplied in parent fxn
  if(is.null(columns)) {

    columns <- purrr::map_chr(rlang::enquos(...), rlang::quo_name)

  }


  ### Group standard data
  std_data_grouped <- ezmmek_std_lm(std_data,

                                    columns = columns,

                                    method = method)


  ### Assign new class
  class(std_data_grouped) <- c("new_ezmmek_std_group", "data.frame")


  std_data_grouped


}
```

Function III-5: *ezmmek_calc_mm_fit*

```r
########
### Calculate nls fit model
########
ezmmek_calc_mm_fit <- function(df,
                               km,
                               vmax) {


  ### If statements to adjust column names
  if("act_calibrated_data_g" %in% colnames(df)) {

    df <- df %>% dplyr::rename(act_calibrated_data = act_calibrated_dat
a_g)

  }


  if("act_calibrated_data_s" %in% colnames(df)) {

    df <- df %>% dplyr::rename(act_calibrated_data = act_calibrated_dat
a_s)

  }


  ### Michaelis-Menten formula
  mm_form <- formula(activity_m ~ (vmax * substrate_conc) /

                       (km + substrate_conc))


  ### Assign starting values to predict km and vmax
  max_activity_m <- purrr::map_dbl(df$act_calibrated_data, function(df)
max(df[[8]]))
  median_substrate_conc <- purrr::map_dbl(df$act_calibrated_data, funct
ion(df) median(df[[1]]))


  ### If km and vmax arguments are NULL, predict km and vmax values
  if(is.null(km) | is.null(vmax)) {


    mm_fit <- nls2::nls2(formula = mm_form, data = df$act_calibrated_da
ta[[1]],
```

```
                             start = list(vmax = max_activity_m, km = media
n_substrate_conc))


    ### Else rely on user defined km and vmax

  } else {


    ### Michaelis-Menten formula

    mm_fit <- nls2::nls2(formula = mm_form, data = df$act_calibrated_da
ta[[1]],

                             start = list(vmax = vmax, km = km))

  }


  ### Create a 1-column data frame with a 'grid' of points to predict
  min_substrate_conc <- purrr::map_dbl(df$act_calibrated_data, function
(df) min(df[[1]]))
  max_substrate_conc <- purrr::map_dbl(df$act_calibrated_data, function
(df) max(df[[1]]))
  pred_grid <- data.frame(substrate_conc = seq(from = min_substrate_con
c, to = max_substrate_conc, length.out = 1000))


  out_list <- list(mm_fit = mm_fit,

                   pred_grid = pred_grid)


  out_list


}
```

Function III-6: *ezmmek_calibrate_activities*

```r
########
### Calibrate activities by standard curve data
########


ezmmek_calibrate_activities <- function(df, method, columns) {


  if(method == "steen") {
    ### Calibrates raw activity data by standard curve
    std_act_calibrated <- df %>%

      tidyr::unnest(act_raw_data_s) %>%

      dplyr::mutate(signal_calibrated = ((signal - kill_control) - std_
lm_homo_intercept) / std_lm_homo_slope) %>% #calibrate signal

      tidyr::nest(act_calibrated_data = c(time, signal, kill_control, s
ignal_calibrated)) %>% #place calibrated signal back in nested df

      dplyr::mutate(activity = purrr::map_dbl(act_calibrated_data,   #ca
lculate slope of calibrated data

                                              function(df) coef(lm(sign
al_calibrated ~ time,

                                                                    data
= df))[2]) * assay_vol) %>%

      dplyr::group_by_at(dplyr::vars(substrate_conc, substrate_type, in
tersect(names(.), columns))) %>%

      dplyr::mutate(activity_m = mean(activity), #calculate means and s
d's of activities

                    activity_sd = sd(activity)) %>%

      tidyr::unnest(act_calibrated_data) %>%

      tidyr::nest(act_calibrated_data_s = c(substrate_conc,

                           replicate,

                           time,

                           signal,

                           kill_control,

                           signal_calibrated,

                           activity,

                           activity_m,
```

76

```r
                                     activity_sd))

  }


  if(method == "german") {

    std_act_calibrated <- df %>%

      tidyr::unnest(act_raw_data_g) %>%

      dplyr::mutate(emission_coef = std_lm_homo_slope / assay_vol, #emi
ssion coefficient

                    net_signal = (signal - homo_control) / quench_coef
- substrate_control, #net signal

                    activity = (net_signal * buffer_vol) / (emission_co
ef * homo_vol * time * soil_mass)) %>% #activity

      dplyr::group_by(substrate_conc) %>%

      dplyr::mutate(activity_m = mean(activity), activity_sd = sd(activ
ity)) %>% #mean and sd of activity

      tidyr::nest(act_calibrated_data_g = c(substrate_conc,

                                            replicate,

                                            time,

                                            signal,

                                            buffer_vol,

                                            homo_vol,

                                            soil_mass,

                                            assay_vol,

                                            homo_control,

                                            substrate_control,

                                            net_signal,

                                            activity,

                                            activity_m,

                                            activity_sd))

  }
  std_act_calibrated
}
```

Function III-7: *ezmmek_std_lm*

```r
########
### Calculate standard curve linear models
########
ezmmek_std_lm <- function(df,
                          method = method,
                          columns = NULL) {


  ### Stop function if method is not assigned approriately
  if(
    !(method == "steen") & !(method == "german")
  ) {
    stop("method must equal 'steen' or 'german'")
  }


  if("std_conc" %in% columns) {
    stop("Cannot group arguments used to calculate linear model ('std_c
onc', 'homo_signal', 'buffer_signal')")
  }


  ### Steen method
  if(method == "steen") {

    ### Require certain column names
    assertable::assert_colnames(data = df,
                                colnames = c("std_conc",
                                             "homo_signal"),
                                only_colnames = FALSE,
                                quiet = TRUE)


    ###### Groups data by user-decided column names
    ######### Creates dataframe containing lm list for each unique set
of grouped column
    std_data_lm <- df %>%
```

```r
      dplyr::group_by_at(dplyr::vars(intersect(names(.), columns))) %>%

      dplyr::group_nest(.key = "std_raw_data_s") %>%

      dplyr::mutate(std_lm_homo_obj = purrr::map(std_raw_data_s, functi
on(df) ezmmek_calc_std_lm_homo(df)), #homogenate lm

                    std_lm_homo_slope = purrr::map_dbl(std_raw_data_s,
function(df) coef(ezmmek_calc_std_lm_homo(df))[2]), #homogenate slope

                    std_lm_homo_intercept = purrr::map_dbl(std_raw_data
_s, function(df) coef(ezmmek_calc_std_lm_homo(df))[1]) #homogenate inte
rcept

    )

  }


  ### German method

  if(method == "german") {


    ### Require certain column names

    assertable::assert_colnames(data = df,

                                colnames = c("std_conc",

                                             "homo_signal",

                                             "buffer_signal"),

                                only_colnames = FALSE,

                                quiet = TRUE)


    ###### Groups data by user-decided column names
    ######### Creates dataframe containing lm list for each unique set
of grouped column

    std_data_lm <- df %>%

      dplyr::group_by_at(dplyr::vars(intersect(names(.), columns))) %>%

      dplyr::group_nest(.key = "std_raw_data_g") %>%

      dplyr::mutate(std_lm_homo_obj = purrr::map(std_raw_data_g, functi
on(df) ezmmek_calc_std_lm_homo(df)), #homogenate lm

                    std_lm_homo_slope = purrr::map_dbl(std_raw_data_g,
function(df) coef(ezmmek_calc_std_lm_homo(df))[2]), #homogenate slope

                    std_lm_homo_intercept = purrr::map_dbl(std_raw_data
_g, function(df) coef(ezmmek_calc_std_lm_homo(df))[1]), #homogenate int
ercept
```

```
                st_lm_buffer_obj = purrr::map(std_raw_data_g, funct
ion(df) ezmmek_calc_std_lm_buffer(df)), #buffer lm

                std_lm_buffer_slope = purrr::map_dbl(std_raw_data_g
, function(df) coef(ezmmek_calc_std_lm_buffer(df))[2]), #buffer slope

                std_lm_buffer_intercept = purrr::map_dbl(std_raw_da
ta_g, function(df) coef(ezmmek_calc_std_lm_buffer(df))[1]), #buffer int
ercept

                quench_coef = std_lm_homo_slope / std_lm_buffer_slo
pe #quench coefficient

      )

  }


  std_data_lm


}
```

Function III-8: *ezmmek_calc_lm_buffer*

```r
########
### Make standard curve lm object for buffer
########


ezmmek_calc_std_lm_buffer <- function(df) {


  ### Fit linear model to buffer
  std_curve_lm_buffer <- lm(formula = buffer_signal ~ std_conc, data =
df)


  std_curve_lm_buffer


}
```

Function III-9: *ezmmek_calc_lm_homo*

```r
########
### Make standard curve lm object for homogenate
########


ezmmek_calc_std_lm_homo <- function(df) {


  ### Fit linear model to homogenate
  std_curve_lm_homo <- lm(formula = homo_signal ~ std_conc, data = df)


  std_curve_lm_homo
}
```

Function III-10: *plot_new_ezmmek_sat_fit*

```r
plot.new_ezmmek_sat_fit <- function(df, ...) {


  ### User-defined columns to facet by
  columns <- rlang::enquos(...)


  ### Plot points without curve fit
  point_plot <- plot.new_ezmmek_calibrate(df, columns = columns)


  ### Unnest predicted activities df
  unnest_sat_df <- tidyr::unnest(df, pred_activities)


  sat_fit_plot <- point_plot +
    ggplot2::geom_line(data = unnest_sat_df,
                       ggplot2::aes(x = substrate_conc, y = activity_m)
) +
    ggplot2::facet_wrap(columns)


  sat_fit_plot


}
```

Function III-11: *plot_new_ezmmek_calibrate*

```r
plot.new_ezmmek_calibrate <- function(df, ..., columns = NULL) {


  ### User-defined columns to facet by if column names not supplied by
parent fxn

  if(is.null(columns)) {

    columns <- rlang::enquos(...)

  }




  ### Correct for different column names with 'if' statements
  ### German protocol

  if("act_calibrated_data_g" %in% colnames(df)) {

    df <- df %>% dplyr::rename(act_calibrated_data = act_calibrated_dat
a_g,

                              std_raw_data = std_raw_data_g)

  }


  ### Steen protocol

  if("act_calibrated_data_s" %in% colnames(df)) {

    df <- df %>% dplyr::rename(act_calibrated_data = act_calibrated_dat
a_s,

                              std_raw_data = std_raw_data_s)

  }


  ### Unnest activity data
  unnest_cal_df <- tidyr::unnest(df, act_calibrated_data)


  ### Make plot of activity data
  cal_plot <- ggplot2::ggplot(data = unnest_cal_df,

                              mapping = ggplot2::aes(x = substrate_conc
,

                                                     y = activity_m)) +

    ggplot2::geom_point() +
```

```
    ggplot2::geom_errorbar(ggplot2::aes(ymin = activity_m - activity_sd
,
                                        ymax = activity_m + activity_sd
)) +

    ggplot2::theme_bw() +

    ggplot2::facet_wrap(columns)


cal_plot


}
```

Function III-12: *plot_new_ezmmek_act_group*

```r
plot.new_ezmmek_act_group <- function(df, ...) {

  ### User-defined columns to facet by
  columns <- rlang::enquos(...)


  ### Use 'if' statements to adjust column names
  ### German protocol
  if("act_raw_data_g" %in% colnames(df)) {

    df <- df %>% dplyr::rename(act_raw_data = act_raw_data_g)


    unnest_act_df <- tidyr::unnest(df, act_raw_data)


    ### Make plot
    act_plot <- ggplot2::ggplot(data = unnest_act_df,

                                mapping = ggplot2::aes(x = substrate_co
nc,

                                                       y = signal,

                                                       color = as.facto
r(replicate))) +

      ggplot2::geom_point() +

      ggplot2::theme_bw() +

      ggplot2::scale_color_discrete(name = "replicate") +

      ggplot2::facet_wrap(columns)


  }


  ### Steen protocol
  if("act_raw_data_s" %in% colnames(df)) {

    df <- df %>% dplyr::rename(act_raw_data = act_raw_data_s)


    unnest_act_df <- tidyr::unnest(df, act_raw_data)


    ### Make plot
```

```r
    act_plot <- ggplot2::ggplot(data = unnest_act_df,
                                 mapping = ggplot2::aes(x = time,
                                                        y = signal,
                                                        color = as.facto
r(replicate))) +
      ggplot2::geom_point() +
      ggplot2::geom_smooth(method = "lm") +
      ggplot2::theme_bw() +
      ggplot2::scale_color_discrete(name = "replicate") +
      ggplot2::facet_wrap(columns)


    }


    act_plot


}
```

Function III-13: *plot_new_ezmmek_std_group*

```r
plot.new_ezmmek_std_group <- function(df, ...) {

  ### User-defined columns to facet by
  columns <- rlang::enquos(...)



  ### German protocol
  if("std_raw_data_g" %in% colnames(df)) {


    homo_plot <- ggplot2::ggplot(data = tidyr::unnest(df, std_raw_data_
g),
                                 mapping = ggplot2::aes(x = std_conc, y
= homo_signal)) +
      ggplot2::geom_point() +
      ggplot2::geom_smooth(method = "lm") +
      ggplot2::theme_bw() +
      ggplot2::facet_wrap(columns)


    buffer_plot <- ggplot2::ggplot(data = tidyr::unnest(df, std_raw_dat
a_g),
                                   mapping = ggplot2::aes(x = std_conc,
y = buffer_signal)) +
      ggplot2::geom_point() +
      ggplot2::geom_smooth(method = "lm") +
      ggplot2::theme_bw() +
      ggplot2::facet_wrap(columns)


    print(homo_plot)
    print(buffer_plot)


    out_list <- list(std_homo_plot = homo_plot,
                     std_buffer_plot = buffer_plot)
    out_list
```

```r
  }


  ### Steen protocol
  if("std_raw_data_s" %in% colnames(df)) {


    ### Make plot
    homo_plot <- ggplot2::ggplot(data = tidyr::unnest(df, std_raw_data_
s),

                                 mapping = ggplot2::aes(x = std_conc, y
= homo_signal)) +
      ggplot2::geom_point() +
      ggplot2::geom_smooth(method = "lm") +
      ggplot2::theme_bw() +
      ggplot2::facet_wrap(columns)


    homo_plot


  }


}
```

CHAPTER IV
CONCLUSION

Extracellular enzyme assays are useful tools for studying microbial ecology, but the practice of broad methodologies inhibits studies from being intercomparable and reproducible. The extracellular enzyme assay protocol has the potential to impact the measurement of key parameters related to enzyme kinetics, notably the K_M and V_{Max} values. *ezmmek* provides a useful platform to compare those impacts reproducibly. Preliminary comparisons suggest that the IBC Protocol may be more error prone than the ISC Protocol, but more robust analyses must be performed before this observation can be considered conclusive. We hope that *ezmmek* will be adopted by enzyme assay practitioners to standardize their methodologies, regardless of which protocol they prefer to use.

L. rhamnosus GG produces L-Leucine aminopeptidases following the ISC Protocol. Under the IBC Protocol, this conclusion would likely remain intact, albeit the calculated activities between protocols could differ by orders of magnitude. At this time, confident recommendations cannot be made as to which extracellular enzyme assay protocol should be applied to MC-LR and other organic matter degradation studies. We suggest that enzyme assay practitioners be explicit about how their activity measurements were collected, in such a way that their results can be reproduced by another party. More confident recommendations may develop in the future, as more robust analyses are performed to compare protocols.

VITA

Christopher L. Cook was born in Maryland and grew up in the city of Havre De Grace. He graduated from Havre De Grace High School before attending Towson University to earn a Bachelor of Science in Geology. He moved to Knoxville, Tennessee, in 2018 to earn a Master of Science in Geology.